Review Article: Melt-Affected Ice Cores for Polar Research in a Warming World

Dorothea Elisabeth Moser[1,2], Elizabeth R. Thomas[1], Christoph Nehrbass-Ahles[2,3], Anja Eichler[4,5], Eric Wolff[2]

[1]Ice Dynamics and Palaeoclimate, British Antarctic Survey, Cambridge, CB3 0ET, United Kingdom
[2]Department of Earth Sciences, University of Cambridge, Cambridge, CB2 3EQ, United Kingdom
[3]Gas Metrology Group, National Physical Laboratory, Teddington, TW11 0LW, United Kingdom
[4]Laboratory of Environmental Chemistry, Paul Scherrer Institute, CH-5232 Villigen PSI, Switzerland
[5]Oeschger Centre for Climate Change Research, University of Bern, CH-3012 Bern, Switzerland

Correspondence to: Dorothea Elisabeth Moser (moser@bas.ac.uk)

Abstract. Melting polar and alpine ice sheets in response to global warming pose ecological and societal risks but will also hamper our ability to reconstruct past climate and atmospheric composition across the globe. Since polar ice caps are crucial environmental archives but highly sensitive to ongoing climate warming, the Arctic and Antarctic research community is increasingly faced with melt-affected ice cores, which are already common in alpine settings of the lower latitudes.

Here, we review the characteristics and effects of near-surface melting on ice-core records focussing on a polar readership and make recommendations for melt-prone study regions. This review first covers melt layer formation, identification and quantification of melt, and structural characteristics of melt features. Subsequently, it discusses effects of melting on records of chemical impurities, i.e. major ions, trace elements, black carbon, and organic species, as well as stable water isotopic signatures, gas record, and applications of melt layers as environmental proxies.

Melting occurs during positive surface energy balance events, which are shaped by global to local meteorological forcing, regional orography, glacier surface conditions and subsurface characteristics. Meltwater flow ranges from homogeneous wetting to spatially heterogeneous preferential flow paths and is determined by temperature, thermal conductivity and stratigraphy of the snowpack. Melt layers and lenses are the most common consequent features in ice cores and are usually recorded manually or using line scanning. Chemical ice-core proxy records of water-soluble species are generally less preserved than insoluble particles such as black carbon or mineral dust due to their strong elution behaviour during percolation. However, a high solubility in ice as observed for ions like F^-, Cl^-, NH_4^+, or ultra-trace elements can counteract the high mobility of these species due to a burial in the ice interior. Stable water isotope records like $\delta^{18}O$ are often preserved but appear smoothed if significant amounts of meltwater were involved. Melt-affected ice cores are further faced with questions about the permeability of the firn column for gas movement, and gas concentrations can be increased through dissolution and in-situ production. Noble gas ratios can be useful tools to identify melt-affected profile sections in deep ice. Despite challenges for ice-core climate reconstruction based on chemical records, melt layers are a proxy of warm temperatures above freezing, which is most sensitive in the dry snow and percolation zone.

Bringing together insights from snow physics, firn hydrology and ice-core proxy research, we aim to foster a more comprehensive understanding of ice cores as climate and environmental archives, provide a reference on how to approach
35 melt-affected records, and raise awareness of the limitations and potential of melt layers in ice cores.

1 Introduction – The importance of studying melting and affected ice cores

Polar ice cores are widely recognised for their ability to archive past climates on local to global and sub-annual to multi-millennial scales (EPICA Community Members, 2004; NEEM community members, 2013; WAIS Divide Project Members, 2013). Beyond the polar regions, ice cores from alpine glaciers, ice fields or lower elevation coastal domes and islands
40 (Fritzsche et al., 2005; Porter et al., 2021; Thomas et al., 2021; Winski et al., 2018) provide an opportunity to reconstruct more local and regional climatic change. Rising global temperatures (IPCC, 2021) and accelerated melting of the most vulnerable parts of the cryosphere (IPCC, 2019) cause glaciers across the globe to shrink, thereby hampering our ability to reconstruct past climate from ice cores across the globe.

On the snow surface of a glacier, melting and refreezing leaves an imprint on the snowpack, i.e. typically cm-thick, bubble-
45 free melt lenses and layers with fuzzy edges (Fig. 1). Wind abrasion, deposition hiatus and other factors, which are still under discussion, can also lead to distinct, mm-thick, high-density bubble-free layers like wind crusts and glaze that are structurally similar to melt layers (Fegyveresi et al., 2018; Frezzotti et al., 2002; Orsi et al., 2015; Weinhart et al., 2021; Zhang et al., 2023), but water is absent during the formation process. Presence and impact of the water phase are what makes melt a major constraint for the selection of ice-core drilling sites. While melting is rare and related alterations of climate indicators are yet
50 of little concern to some researchers working on ice cores from central Antarctica, key climate proxy records like $\delta^{18}O$ have already been obliterated through melting in numerous low-latitude high-altitude glaciers (Thompson et al., 2021) and are gradually deteriorating at (sub-)polar sites like Svalbard (Spolaor et al., 2023). Unlike the original climate signatures preserved under dry conditions, palaeoclimate reconstructions based on ice cores from melt-affected drilling sites require caution and have been hampered by insufficient knowledge about the effects of melting on ice-core proxy records and how to correct for
55 them in the past. In recent decades, alpine ice-core scientists faced with this issue regularly have made significant advances regarding the interpretation of melt-affected ice-core records (Avak et al., 2018). Improvements have also been made on the wider subject of snow melt with interdisciplinary methodical approaches ranging from detection with remote sensing (Alimasi et al., 2020; Bell et al., 2017; Dell et al., 2021) to field-based snow pits (Avak et al., 2019; Moran & Marshall, 2009; Spolaor et al., 2021), firn sintering and elution experiments (Cragin et al., 1996; Trachsel et al., 2019), modelling (Zhongyang et al.,
60 2021), and ice-core studies (Avak et al., 2018; Orsi et al., 2015; Vega et al., 2016). Yet among polar ice-core scientists, still only limited agreement exists about the informational value of melt-affected ice cores: On the one hand, chemical records of refrozen melt layers are often considered lost or altered, and likely to lead to misinterpretations of proxy records (Koerner, 1997). On the other hand, these structural features have been used as proxies for warm summer temperatures in multiple studies from the Arctic and Antarctic (Abram et al., 2013; Das & Alley, 2008; Koerner & Fisher, 1990).
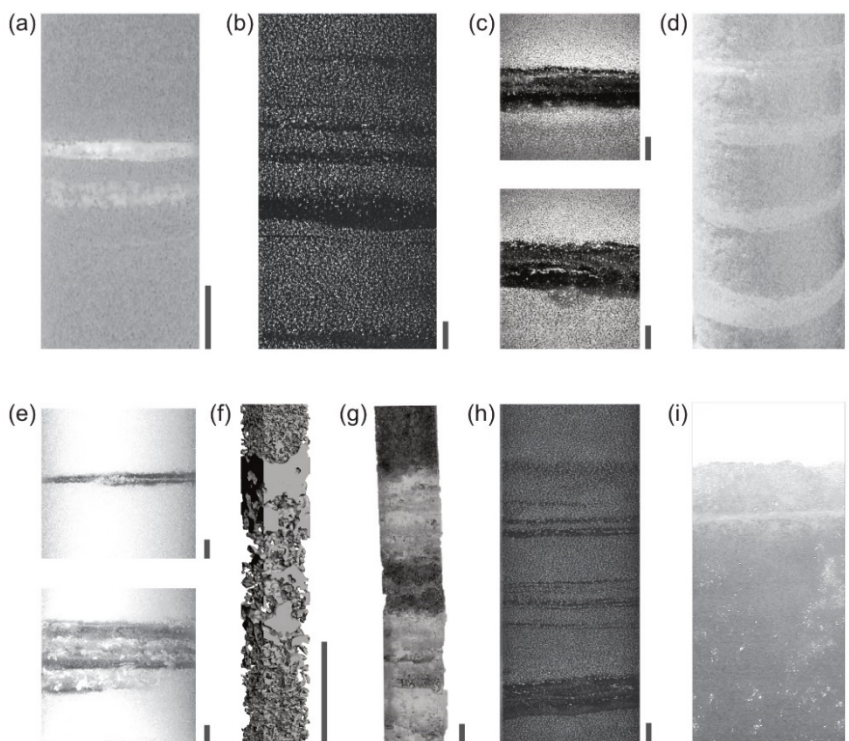
Figure 1: Examples of melt layers reported in snow and ice profiles from around the world using various techniques; the grey scale bar at the bottom right of each panel equals 1 cm, and the top of each snow/firn/ice section is at the top of each panel: a) two melt layers, 4–6 mm thick, from the NEEM Greenland ice core at ~44.3 m depth (digital photo, credit Kaitlin Keegan, Orsi et al., 2015); b) sequence of melt layers ranging 3–13 mm at EastGRIP, Greenland ice core at ~138.04 m depth, (line scan image, Westhoff et al., 2022, CC-BY 4.0); c) two distinct melt layers ~15-20 mm thick at RECAP, Renland Ice Cap, at 78.1–79.2 m depth (line scan image, Taranczewski et al., 2019); d) four ~20–35 mm melt layers at 0.3–0.5 m depth in an ice core from the Agassiz Ice Cap, Canada (digital photo, credit James Zheng, Fisher et al., 2012, reproduced with permission from Elsevier); e) varying appearance of 3–7 mm and 25–41 mm melt layers in an ice core from Mount Hunter, Alaska (digital photo, Winski et al., 2018); f) ~15–20 mm melt at ~0.04 m depth in surface snowpack from Davos, Swiss Alps (3D X-ray tomography scan, Heggli et al., 2011); g) segment at ~3 m depth from the Young Island ice core with melt >45 mm thick (digital photo, Moser et al., 2021, CC-BY 4.0); h) melt sequence between 133.82–1.92 m depth in ice core from James Ross Island, Antarctic Peninsula (line scan image, Abram et al., 2013, reproduced with permission from SNCSC); i) a 1-mm melt layer in the surface snow at 0.008 m depth at Siple Dome, Antarctica (digital photo, Das & Alley, 2005).

In the past, studies about melt in ice cores were focussed on alpine settings (Avak et al., 2018; Eichler et al., 2001; Kang et al., 2008; Yuanqing et al., 2001). Such mountain glaciers around the Earth are vanishing (IPCC, 2019), because a rise in local equilibrium lines driven by global heating exposes most of their surfaces to melt as a cause of ablation. At the extreme end, the fear that melt may make ice cores from some sites unusable has motivated the Ice Memory Initiative (Ginot et al., 2021). Among (sub-)polar ice-core researchers, increasing temperatures have sparked interest in drivers of snow melt and firn hydrology in the Arctic and Antarctic, where the firn is generally cold even though melting may occur. For example, in Greenland, the extensive melt event in 2012 (Nghiem et al., 2012) was followed up by record-melt in 2019 (Tedesco &

Fettweis, 2020) and rain-driven melt reached Greenland Summit in August 2021 (Box et al., 2022). The increase in Greenland ice sheet melting (IPCC, 2019) and rainfall (Niwano et al., 2021) is expected to continue in a warming climate. Even in Antarctica, recent melt events (Nicolas et al., 2017) have raised concerns about a reduction of firn refreezing capacity, potential hydro-fracturing and ice shelf instability (Bell et al., 2017; Gilbert & Kittel, 2021; Munneke et al., 2014; Wille et al., 2019). Surface melt events are rare in Antarctica and mostly restricted to the Antarctic Peninsula (Van Wessem et al., 2016), coastal (Nicolas et al., 2017), low-elevation sites (Thomas et al., 2021) and ice shelves (Banwell et al., 2021; Zou et al., 2021). However, those regions are most sensitive to climate change, and assessing the frequency and characteristics of Antarctic and sub-Antarctic melt events is crucial to constrain the (surface) mass balance of Antarctica and future sea level rise at large. In addition, the amplified warming of the polar regions is expected to continue and even accelerate depending on the greenhouse gas concentration trajectories in the next few decades (Trusel et al., 2015). Though total surface melting seems to have decreased slightly in the Antarctic Peninsula in the first two decades of the 21st century, winter melt events are becoming more frequent (Zheng et al., 2020), and the global temperature rise leading to melt will affect a growing number of alpine to polar ice-core drilling locations, more frequently, with larger intensity, and at higher elevation further inland (Clem et al., 2020; Gilbert & Kittel, 2021; Nicolas et al., 2017; Winski et al., 2018).

Bridging the gap between alpine expertise on how to handle melt in ice cores and less melt-acquainted polar ice-core scientists is urgently needed, because understanding the drivers of recent climate changes, in particular increased melt and melt-driven changes in Antarctic mass balance is paramount. With increasing interest in the role of sea ice (Thomas et al., 2019), atmospheric circulation (Wille et al., 2019), and tropical teleconnections (Nicolas et al., 2017), the research field is increasingly looking to the fringes of the Antarctic ice sheet. The demand for (sub-)polar ice-core profiles from low elevations, coastal and island regions means that effects of melt on ice-climate proxy records cannot always be avoided. The polar ice-core community urgently needs to prepare for ice-core science under warming conditions.

It is the aim of this review to bring together insights from snow physics, firn hydrology and ice-core proxy research in order to present the status quo on the influence of melt on ice proxy preservation, and subsequently make suggestions for future projects in melt-prone study regions. This paper provides a detailed literature review regarding external drivers of melt events (Sect. 2.1); physics of melt layer formation and behaviour during snow metamorphism (Sect. 2.2); identification and quantification of melt (Sect. 2.3); structural characteristics of melt features (Sect. 3.1); effects of melting on records of chemical impurities, i.e. major ions, trace elements, black carbon (BC), and organic species (Sect. 3.2), stable water isotopic signatures (Sect. 3.3), and gas record (Sect. 3.4); applications of melt layers as environmental proxies (Sect. 3.5). Here, we review formation, manifestation, and interpretation of melt chronologically and focus on those aspects of near-surface melting, which are important for ice-core research. Englacial or basal melt phenomena as well as glacier-wide melt assessment based on remote sensing are beyond the scope of this study. Finally, this study aims to learn from alpine ice-core scientists and contribute to a more comprehensive understanding among polar researchers of the limitations and potential of melt features in ice cores.

2 From melting to melt-affected ice cores

2.1 Drivers of melt

Generally, melting takes place whenever sufficient energy is available to cause a phase change from ice to water. The components of this surface energy balance (SEB) contributing to this surplus can be expressed as shown in the following Equation (Eq. 1):

$$M = SW_{\downarrow} - SW_{\uparrow} + LW_{\downarrow} - LW_{\uparrow} + H + L + R + G \tag{Eq. 1}$$

where M denotes the energy available for heating ice at sub-zero temperatures or melting temperate ice, SW refers to incoming ($\downarrow$) and outgoing ($\uparrow$) shortwave radiation; LW is longwave radiation; turbulent fluxes comprise sensible heat flux (H) and latent heat flux of water vapour (L); R is the sensible energy supplied by rain, and G is the ground heat flux. Numerous studies have assessed the surface energy balance and how to model the underlying processes (Hock, 2005). Here, we focus on the environmental context of the SEB, because each component of the SEB is driven by global-to-local meteorological forcing (Kinnard et al., 2008) and its interactions with the surface and sub-surface properties of the glacier (Fig. 2).
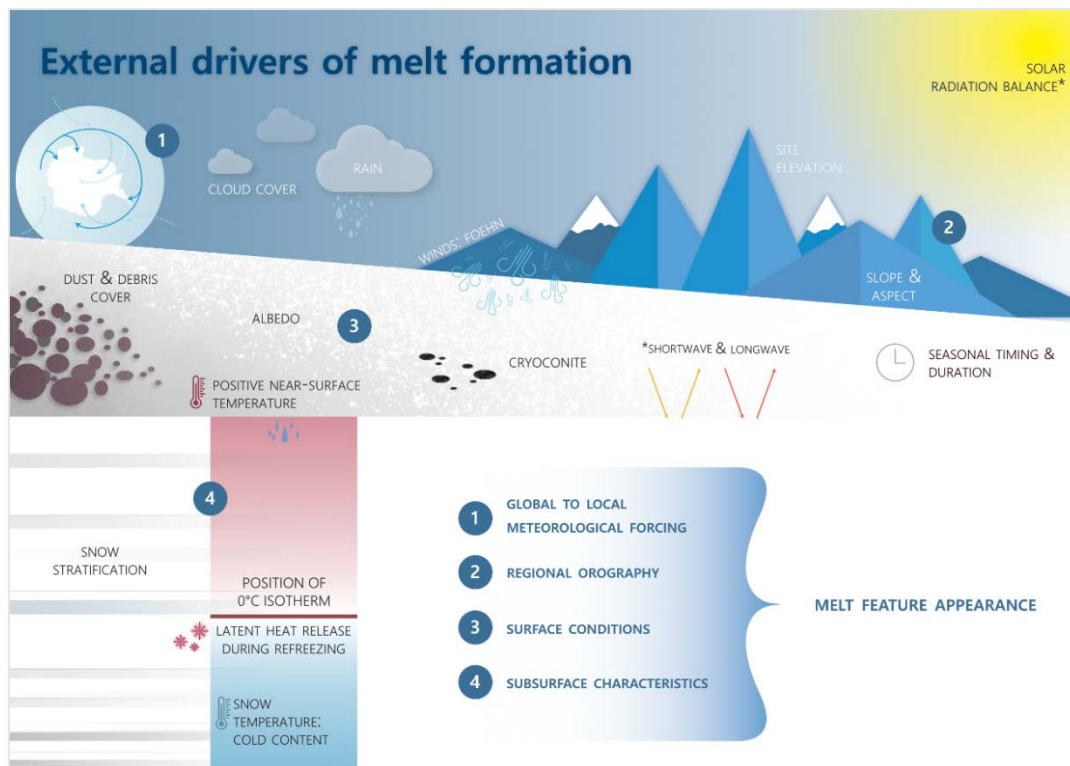
Figure 2: Schematic overview of the diverse, external drivers and constraints of near-surface snow melt discussed in Sect. 2.1, including global to local meteorological forcing, regional orography, surface conditions, and subsurface characteristics.

Positive air temperatures are the primary, non-linearly related trigger of melt and a well-established, integrated proxy for melt intensity (Abram et al., 2013; Hock, 2003; Bell et al., 2018). Warm air can be linked to various components of the SEB. Melt rates of up to 4 mm water equivalent (w.eq.) per day have been recorded on the Eastern Antarctic Peninsula, attributed to warm air advection in combination with foehn wind effects (Van Den Broeke, 2005). Warm air advection is shaped by synoptic-scale atmospheric circulation patterns like high-pressure blockages, which facilitate moist-warm air intrusions (e.g. West Antarctic Ice Sheet, WAIS, Scott et al., 2019). Similar importance of atmospheric blocking has been observed for Greenland melt (Hanna et al., 2013, 2014; McLeod & Mote, 2016). Linear-shaped air intrusions are often referred to as 'atmospheric rivers' and correlate highly with melt production in both Greenland and Antarctica (Neff, 2018; Wille et al., 2019). The association is especially strong in Antarctica during winter (Wille et al., 2019), and for example, an atmospheric river is considered responsible for the observed extensive melt in West Antarctica in 2016 (Wille et al., 2019).The atmospheric forcing of melt events also includes near-surface winds (Cullather & Nowicki, 2018). Foehn events are characterized by clear-sky shortwave radiation together with advection of warm, dry air and occur episodically by gravity winds on the lee slopes of mountain ranges like the Antarctic Peninsula (Elvidge & Renfrew, 2016). These foehn winds are coupled to position and strength of the circumpolar westerly wind belt (Datta et al., 2019) and can lead to spatially inhomogeneous melt events (Bell et al., 2018). Melting can also be caused through the 'blanketing effect' of a cloud cover (Cullather & Nowicki, 2018; Hahn et al., 2020; Scott et al., 2019), which increases the down-welling longwave radiation balance. In this regard, altitude and phase-type of the clouds prevailing at the site play a key role for the net radiation effect. Low-altitude, mixed-phase clouds warm the glacier surface, and vice versa.

Such meteorological constellations in the Antarctic are dynamically tied to the climate of the tropics (Winski et al., 2018). When examining melt in ice cores, even such long-distance teleconnections should be taken into account. For example, the strength and position of the Amundsen Sea Low (ASL) is coupled to tropical climate through the El Niño/Southern Oscillation (ENSO) teleconnection, and summer melt in West Antarctica has been linked to strong El Niño (Nicolas et al., 2017; Wille et al., 2019).

Besides the meteorological and climatological drivers of melt events, the regional-to-local shape of an ice body determine its melt response. As the lateral and vertical extent of an ice sheet affects the trajectories of air-masses circulating around it, ice sheet geometry is to be considered a factor for melt occurrence (Das & Alley, 2008). Melt conditions can also vary across short distances, because the regional-scale meteorological drivers described above interact with local site characteristics (Fig. 2). Glacier orography including slope, aspect, and elevation plays a significant role for the local SEB (Arnold et al., 2006; Hahn et al., 2020; Olson & Rupper, 2019). For example, the warming of katabatic winds during its downflow has been shown to enhance melt production especially at the grounding line of an East Antarctic glacier during summer, facilitated by positive wind-albedo and melt-albedo feedbacks through the exposure of blue ice and bedrock (Bell et al., 2018; Lenaerts et al., 2017).

Melt is further driven by site-specific surface snow characteristics (Fig. 2). Snow exposed at the surface undergoes processes like wind-driven redistribution, temperature-gradient and isothermal metamorphism, which alter the size and shape of the deposit and in turn surface albedo. While fresh snow exhibits albedo values of ~0.8, aged snow shows lower values around 0.4 (Dirmhirn & Eaton, 1975) and dirty snow even lower values <0.2 (Conway et al., 1996; Warren, 2019). Thereby, albedo is coupled to melt by positive feedback (Thackeray & Fletcher, 2016), i.e. a lowering of the surface albedo reinforces the tendency for melting and leads to a further albedo decrease. For example, forest fires produce significant amounts of BC and reduce the surface albedo even at distant sites like interior Greenland, a coupling that is expected to increase with climate change (Keegan et al., 2014). Also, debris cover and cryoconite (Fountain et al., 2004), dark-coloured dust containing soot and microorganisms, can lower the albedo and enhance local melt production (Mattson et al., 1993). A debris cover can also act as an insulating active layer, if it is sufficiently thick (Reznichenko et al., 2010; Rowan et al., 2021).

All of this shows that the drivers of a positive SEB and melt events are not uniform. They must be assessed for individual sites and ice-core records within their respective, complex climatic context. The details of the melt process and its sub-surface progression shall be discussed in Sect. 2.2.

2.2 Physics of melt layer formation and dynamics during snow metamorphism

The analysis of melt-affected ice core records is preceded by understanding the physicochemical process of melting ice, which has been investigated extensively since the 19th century (Faraday, 1859; Sánchez et al., 2017). Sánchez et al. (2017) recently presented evidence that melting takes place in a 'bilayer-by-bilayer' fashion leading to a nanometre-thick quasi-liquid layer (QLL) at the ice-air interface (Slater & Michaelides, 2019). As these features already exist within the ice matrix on a grain scale at temperatures below the melting point of the wider snowpack, they are also called 'pre-melting' (Bishop et al., 2009).

On a larger scale, the surface snow starts to melt when the energy balance is positive sufficiently long enough to raise at least parts of the ice matrix to 0°C, and it ends when the energy balance below the 0°C isotherm is negative again. This duration threshold is reached within a few hours to less than a day, as has been recorded for Hansbreen in Svalbard by Laska et al. (2016). Therefore, modelling of melt processes must aim for hourly or at least sub-daily resolution. Furthermore, Koh and Jordan (1995) have shown that radiation-forced temperature maxima and melting can occur a few centimetres below the snowpack surface, especially in low-density snow. Since the surface energy conditions vary significantly over short time scales, e.g. during diurnal cycles, 'melt-freeze' features (referred to as melt features hereafter) tend to develop accordingly (Colbeck, 1982).

Melting leads to wet metamorphism, during which liquid water is available and acts as a carrier of thermal energy, which accelerates post-depositional alteration of the affected snow layers. Wet metamorphism is generally isothermal (Brun, 1989; Wakahama, 1968, 1975), characterized by a rise in grain size and density caused by recrystallization, and increasing liquid water content softens the snow (Colbeck, 1982). This process leads to the key structural characteristics of melt features in ice cores, which is discussed in Sect. 3.1.

Melt generated near the snow surface can penetrate into the underlying snowpack (Westhoff et al., 2022). The progression of the percolation front depends on local thermodynamic and hydrological conditions and has been modelled and observed to varying degrees from alpine to polar sites (Graeter et al., 2018; Meyer & Hewitt, 2017). Meltwater infiltration into deeper, older snow makes percolation a secondary process leading to mixed snow compositions and climatic signatures, e.g. of summer melt in winter snow (Moore et al., 2005). For similar reason, infiltration beyond the current annual layer is an issue when interpreting ice-core proxy and melt layer records, so that using multi-year averages of melt indices has been recommended previously (Graeter et al., 2018). Furthermore, positive-degree-day (PDD) sums are a common tool to quantify ablation due to temperatures above melting point (Hock, 2003). With PDD values normalized to a single day (°C-day), Das and Alley (2005) have estimated +5.22°C as the temperature for a West Antarctic site, above which it is probable that percolation of a single melt event reaches into accumulation of the previous year. However, this parameter requires site-specific assessment. The rate of melt production further governs the exposure period of snow to melt liquid (Taylor et al., 2001) through the 'saturation, refreezing capacity, and drainage processes' within the firn (Samimi et al., 2020). This is important when it comes to interpreting chemical records from melt-affected ice cores.

In addition to the energy balance at the snow surface and gravitation in general, speed and type of meltwater flow are determined by characteristics of the subsurface including (1) temperature, (2) thermal conductivity and (3) stratigraphy of the snowpack. (1) Cold subsurface temperatures of the snowpack, the so-called 'cold content', are a strong constraint for snowmelt production (Jennings et al., 2018). Depending on the cold content, large amounts of energy might be needed to raise the snow temperature to melting point and delay the progression of the melting front at the 0°C isotherm to deeper layers. (2) According to Pfeffer & Humphrey (1998), the balance between melting and refreezing is also driven by thermal conductivity of the ice matrix, which in turn depends on firn density. High densities allow for more freezing, and vice versa. (3) Snow column stratigraphy affects the direction of flow through capillary and hydrological forces. Neighbouring snow deposits can differ significantly in terms of microstructure, e.g. grain size and porosity, and so do their capillary characteristics and permeability. It is due to this difference in capillary resistance that fine-to-coarse transitions are well known to retard vertical meltwater percolation (Pfeffer & Humphrey, 1996), but differences in capillary characteristics can lead to lateral meltwater suction, too. McDowell et al. (2023) have recently identified a two-way feedback between pre-existing microstructural transitions in firn, which facilitate melt infiltration and wet metamorphism locally, and more ice layers but fewer fine-over-coarse transitions in firn cores after melt-induced metamorphism. Hydrological barriers can also be high-density layers like wind crusts (Das & Alley, 2005) or pre-existing melt layers (Samimi et al., 2020), and both are frequent features in alpine to polar settings. Furthermore, progression of melt is not only halted by fully melt-filled refrozen pores but by closed pore connections (Humphrey et al., 2021). Taken together, snow conditions constraining the flow are expected to lead to sharper contacts between melt layer and adjacent firn.

Based on these factors, which determine the flow path of least resistance, percolation take place in different ways (Hirashima et al., 2019). Homogeneous wetting, also known as matrix flow, tends to occur in temperate snow with less dominant

stratigraphic boundaries, and the thawing front progresses laterally uniformly. While at colder, stratigraphically complex sites, lateral and vertical flow alternate spatially and temporally (Pfeffer & Humphrey, 1996; Williams et al., 2010). Preferential flow takes place where meltwater flow instabilities occur at the wetting front (Hirashima et al., 2014, 2017; Leroux & Pomeroy, 240   2017; Parlange, 1974). In this case, capillary pressure of advancing vertically exceeds the capillary pressure of expanding laterally. Dye experiments have frequently been used to visualise this stepwise advance of preferential flow paths (PFPs) along the stratigraphy (Avanzi et al., 2016; Clerx et al., 2022). They also highlight where melt layers don't form directly at the surface but at greater depth. At Neumayer Station in Dronning Maud Land, meltwater has been documented to refreeze 50– 100 cm below the snow surface during summer (Kaczmarska et al., 2006). Given that the flow conditions are a continuum 245   between these two extremes and vary widely among sites and seasons, different structural characteristics of melt in ice cores must be expected (Sect. 3.1). Furthermore, ice cores only capture a very small area, and whether the derived melt records are representative should be corroborated with larger-scale stratigraphic analyses of the sub-surface, e.g. using multiple snow trenches or ground-penetrating radar.

250   Other general physical implications of melting for glaciers and glaciology include: Melt-freeze cycles change the thermal structure within the snowpack, i.e. (sub-)surface warming (Humphrey et al., 2012; Mattea et al., 2021), because freezing 1 g of water raises the temperature of 160 g adjacent snow by 1°C through the release of latent heat (Cuffey & Paterson, 2010). In extreme cases, this can lead to the development of highly permeable firn aquifers (Koenig et al., 2014; Kuipers-Munneke et al., 2014; Miller et al., 2020). In addition, meltwater percolation, especially through PFPs, advects heat to deeper, sub-zero 255   snow sections. At sites with preferential percolation, borehole temperatures can therefore be ambiguous (Pfeffer & Humphrey, 1996).

Since melt complicates firn densification through metamorphism rates differing between affected and unaffected sections, linear densification curve fits solely dependent on the overlying snow burden (Herron & Langway, 1980) are not sufficient to 260   predict internal density variations caused by melt. Improved understanding of firn meltwater retention (Vandecrux et al., 2020) and densification models (Ligtenberg et al., 2011) are therefore crucial, and differences in temporal resolution between unaffected firn and melt layers need to be taken into account when interpreting melt-affected ice cores (Moser et al., 2021). Refrozen melt layers further reduce the permeability of the snow column, i.e. acting as impermeable barriers to percolation. The development of a stratigraphic boundary in turn encourages more ice aggregation at the top and/or bottom of the ice layer 265   and reinforces this effect. Though pneumatic testing has potential to uncover horizontal and vertical firn permeability in situ (Sommers et al., 2017), the effective permeability of refrozen melt layers for percolation is under debate. On the one hand, they can be partly permeable when warmed to melting point and allow for meltwater penetrating beyond these features (Lliboutry, 1996; Samimi et al., 2020). On the other hand, thick ice slabs are expected to be impermeable, because heat transfer in temperate, saturated firn is low (Samimi et al., 2020). Though the development of impermeable ice slabs leads to temporary

270 retention of melt, it also may reduce the firn's capabilities for meltwater storage (Vandecrux et al., 2019) and enhance runoff (Machguth et al., 2016; Pfeffer et al., 1991).

2.3 Identification and quantification of melt

2.3.1 Melt feature records from ice cores

In ice cores, past near-surface melt events are commonly identified as visually distinct features that have been buried within
275 the profile (Fig. 1). Distinction is either made manually during ice core processing in the cold laboratory, where some melt layers can be clearly seen by eye or using line scanners (Brown et al., 2023; Dey et al., 2022; Kinnard et al., 2008; Svensson et al., 2005). Thus, long-term melt history records from Canada (Koerner & Fisher, 1990), Greenland (Westhoff et al., 2022), Alaska (Winski et al., 2018), Arctic Russia (Fritzsche et al., 2005), and the Antarctic Peninsula (Abram et al., 2013) have been acquired.

280 Traditionally, the description of firn sections with melt features tends to be binary as sections 'affected' or 'unaffected' by melt. The resolution ranges between micrometres to a few millimetres, depending on sight or camera capabilities. An issue with this and other structural identification approaches is their inability to discriminate between very thin melt layers and other fine, high-density, bubble-free features like glaze (Albert et al., 2004; Fegyveresi et al., 2018; Frezzotti et al., 2002) and wind crusts (Sommer et al., 2018; Weinhart et al., 2021). While their discrimination requires further investigation, Westhoff et al.
285 (2022), for example, applied a thickness threshold of 1.5 mm as upper limit for wind crusts and considered features >1.5 mm melt-induced.

Furthermore, two melt section of equal thickness imply equal intensity of the melt events, even though various factors shape melt layer appearance (Sect. 2.1 & 2.2). Thickness-based melt estimates don't reflect this complexity and have been shown to significantly overestimate melt proportion in comparison to melt constrained by line-scan derived density (Dey et al., 2022).
290 Both visual processing and line scanning are limited to air bubble containing ice in the topmost few hundred metres of ice above the bubble-to-clathrate transition zone (Neff, 2014), within which the air bubbles start to disappear as the air starts to form clathrates. Within this transition zone the visual differences between melt and non-melt sections (bubble density) vanish. However, this is generally not an issue for shallower, alpine ice cores and only relevant to deep polar ice cores.

Limitations inherent to the features are that (1) both rain-on-snow events and a non-accumulative positive surface energy
295 balance can cause identical features in ice cores; (2) it remains unclear whether a thick melt feature with internal variability resulted from one larger melt phase or several shorter events (Fig. 1); (3) it has been shown that melt percolation of a single event can lead to several melt horizons (Westhoff et al., 2022). Given that ice cores are single-point records of highly dynamic and spatially heterogeneous environments (Zuhr et al., 2021), their representativity must be validated locally and obtained melt history records must be interpreted with caution. Quantitative melt estimates are commonly derived from the frequency and
300 thickness of melt layers. Here, thinning of melt features due to burial-induced densification and glacier flow need to be taken into account. A first melt parameter that does so is 'melt frequency' (MF), defined as number of melt events per depth (metre)

or time unit (Alley & Anandakrishnan, 1995; Kaczmarska et al., 2006; Kinnard et al., 2008). This melt frequency can be used for calculating a second parameter, 'melt features percent' (MFP, Equation 2), i.e. the percentage of melt-affected ice (M_{ice}) of the annual layer (A) in terms of mass (Koerner, 1977a; Winski et al., 2018). The thickness-based approaches will lead to different profiles of the derived melt quantity (Supplementary Table 1).

$$MFP = M_{ice} \div A \times 100 \qquad\qquad \text{(Eq. 2)}$$

Besides the structural identification, chemical characteristics can be used to identify melt layers in ice cores. Methods based on the magnesium-sodium ratio (Li et al., 2006; Watanabe et al., 2015), chloride-sodium ratio (Eichler et al., 2001), trace-element concentration ratios (Avak et al., 2018), dissolved ion fraction percentage (Wu et al., 2018), and radionuclide content (Pinglot et al., 2003) help to identify melt and constrain its effects. Rod-like inclusions (>30 µm) in ice layers have recently been suggested as indicator of large amounts of refrozen meltwater (Kawakami et al., 2022). Total air content, and in particular noble gas measurements have even proven valuable to detect melt where it generally can't be detected visually like in deep, clathrated ice (NEEM community members, 2013; Orsi et al., 2015).

2.3.2 Modelling and remote sensing: potential and limitations for melt identification

Various modelling and remote sensing approaches for the identification and quantification of melt exist, which can support ice core studies in the field. Hock (2005) have previously reviewed different types of melt models using the SEB. Such SEB models have great potential but are sometimes hampered by a lack of meteorological data beyond temperature. Simpler PDD models based on the relationship between melt and temperature (Krenke & Khodakov, 1966) are more commonly applied. However, they struggle to implement the small-scale spatial complexity of melt in heterogeneous topography as well as the continuously changing meteorological and snowpack conditions, which hinders the detailed depiction of melt events.
Remote sensing has become a very influential way to assess melt occurrence in Antarctica, because it allows to investigate for large spatial coverage in the most remote region on Earth. Optical imagery (e.g. Landsat 8, Sentinel-2) and passive microwave sensors, which rely on the change of dielectric properties at the glacier surface (e.g. ICESat-2), are widely used today (Dell et al., 2021; Fricker et al., 2021). The short time span of such satellite observations (max. since 1980s) is a significant limitation for studying changes in climate that take place on decadal to centennial time scales. Furthermore, the detection of surface melt events is directly dependent on the method sensitivity and chosen threshold, which can lead to the confusion of fresh melt events with retained subsurface liquid (Dell et al., 2021).

3 Manifestations of melt in ice-core records

3.1 Structural characteristics of melt features in ice cores

Melting near the snow surface leaves a physical imprint on the stratigraphy of the glacier. Here, we discuss the appearance of melt features in snow, firn and bubbly ice, where structural differences are visible (Fig. 1). As these melt features are buried under new layers of snow, they participate in the snow/firn densification process as well as ice thinning at greater depth. Melt features in deep ice, where high hydrostatic pressure forces air bubbles into clathrates and bubble-free melt sections are practically impossible to detect visually, are addressed in Sect. 2.3.1 and Sect. 3.4.

Similar to glacier hydrology studies (Bell et al., 2018), which describe a variety of surface melt features on a macroscopic scale, it must be noted that traces of melt in ice cores can differ greatly (Fig. 1). A first common characteristic of melt-affected ice-core sections is their distinctly higher density caused by wet metamorphism speeding up the compaction of the snowpack. This corresponds to lower porosity and permeability than the adjacent firn. Secondly, melt features generally contain few air bubbles (Das & Alley, 2005; Langway & Shoji, 1990; Orsi et al., 2015). While some studies state that melt layers are entirely bubble-free, some include bubble-sparse (Ahn et al., 2008; Koerner, 1989) or very coarse-grained yet bubble-containing sections in their definition of melt-affected ice (Macdonell et al., 2021). Depending on the speed of melt infiltration and freeze-off, the degree of degassing in the affected firn has been suggested to vary, i.e. slower freeze off allows for more degassing and consequently fewer, smaller air bubbles in the melt-affected section (Ahn et al., 2008). Therefore, under rapid percolation, air from the open-porous firn can get trapped and merge to enlarged, irregular-shaped bubbles during the freezing process. These differ from regular air bubbles, unaffected by melt, which stem from long-term metamorphism and tend to have a more circular shape resulting from specific surface area reduction.

The impact of recrystallization on granulometry during melt phases has been used by Macdonell et al. (2021) to categorize melt layers as fine (<1 mm), medium (1−2 mm), or large-grained (>3 mm). Another parameter to describe melt features in greater detail are their boundaries to the neighbouring firn. While many polar studies describe sharp contacts between non-melt and melt-affected sections (Das & Alley, 2005), irregular boundaries have also been observed (Fritzsche et al., 2005). Macdonell et al. (2021) observed 'diffuse, sinuous, and planar' contacts. The factors determining between homogeneous wetting and preferential flow, e.g. cold content and stratigraphy of the snowpack (Sect. 2.2), also drive melt layer prominence (Culberg et al., 2021).

While melt layers are frequently reported as 'sub-horizontal' in ice cores with a limited sampling area, the different meltwater flow regimes discussed in Sect. 2.2 can lead to both horizontal and vertical features. Lateral flow is responsible for both discontinuous melt lenses and extensive melt layers (Das & Alley, 2005). Lateral connectivity of melt features is a useful parameter to describe the different degrees of melt impact on the snow stratigraphy, even at a glacier scale (Culberg et al., 2021). At the same time, even when ice layers are continuous across a core, they cannot be assumed to be horizontally uniform (Kameda et al., 1995), and observations from a single ice core are not necessarily representative of the regional melting conditions.

Typical estimates for melt layer thickness are in the range of mm to dm (Das & Alley, 2005; Langway & Shoji, 1990; Orsi et al., 2015), but their extent varies according to the site-specific, short-term meteorological and snowpack conditions. At Site J, southern Greenland, ~38% of melt layers were ≤2 mm thick (Kameda et al., 1995), with features up to 210 mm raising the mean melt thickness to ~10.8 mm. Thereby, 20–100 mm clusters of melt features are common within the ice cores from Site J (Kameda et al., 1995). In a Belukha ice core from the Siberian Altai, melt layers are mostly <10 mm thick with a few outliers >40 mm (Okamoto et al., 2011). Up to 85-mm thick ice layers have been recorded in an ice core from Mt. Yulong on the south-eastern Tibetan Plateau (Yuanqing et al., 2001). Melt features in the first sub-Antarctic ice core from Young Island are on average 64 mm in thickness with a maximum of 580 mm (Moser et al., 2021; Thomas et al., 2021). At James Ross Island, Antarctic Peninsula, the mean vertical extent of melt layers is 32 mm (Abram et al., 2013).

These examples highlight two issues of melt layer records from ice cores: (1) whether close clusters of melt layers and interlayering of ice and firn are counted individually or collectively as one thicker melt-affected section is subjective to the processing team and can vary based on the eyesight or sample cut; (2) whether thick melt features are the result of a single heavy melt event or a sequence of smaller melt events is indistinguishable during ice-core processing and requires further investigation of their internal stratigraphy.

Vertical melt features, so-called melt pipes or flow fingers, are direct evidence of percolation and distinct pathways for liquid beyond the 0°C wetting front (Pfeffer & Humphrey, 1998; Williams et al., 2010). Previous assessments of their diameter summarized by Williams et al. (2010) range from ~36 mm (Marsh & Woo, 1984), generally 50−150 mm and ≤10 mm for low-intensity events early in the season (McGurk & Kattelmann, 1988) to 10−400 mm (Campbell et al., 2006). Their spacing is irregular with estimates ranging from every 30 to 60 mm to hundreds of millimetres in between. Due to their limited horizontal extent, these features are hard to depict in ice cores with a diameter ≤10 cm. Furthermore, stratigraphic boundaries can cause discontinuities of vertical flow features (Williams et al., 2010).

After all, the diverse appearance and structural characteristics of melt features in ice cores are not only influenced by the meteorological and energy balance conditions at the glacier surface but strongly depend on the subsurface characteristics, which determine meltwater flow (Fig. 3).
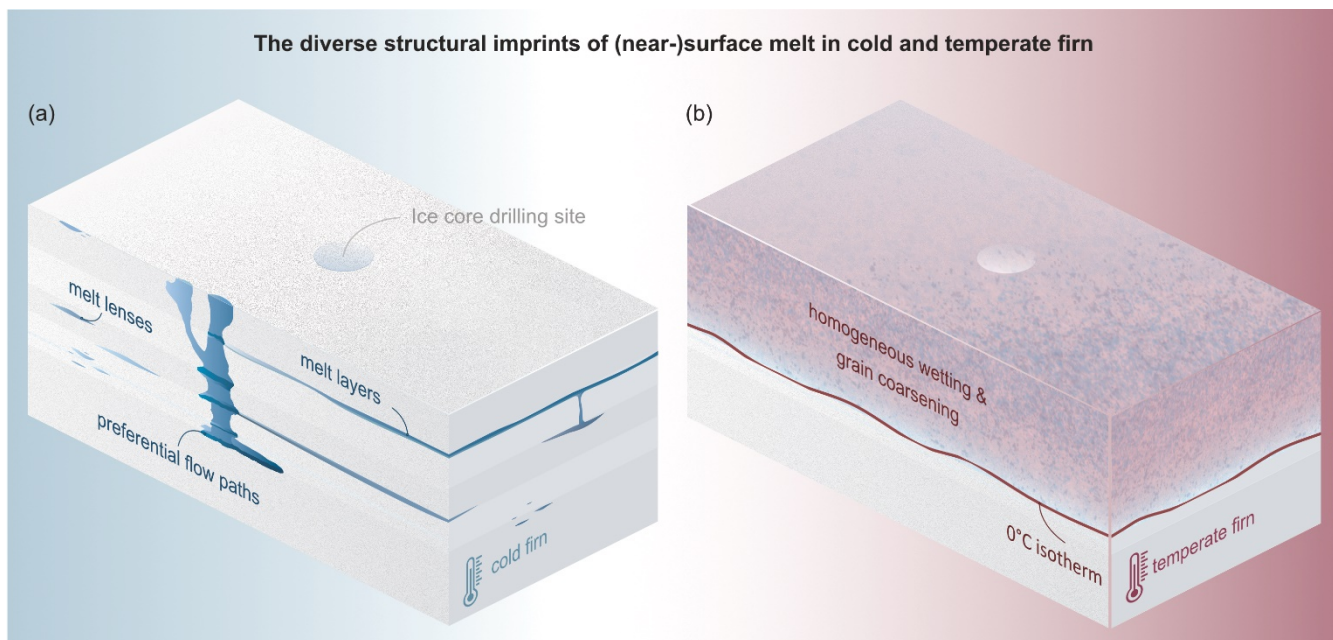
Figure 3: Examples of structural imprints of melt for the extreme scenarios of (a) cold firn and (b) temperate subsurface. Subsurface temperatures influence the meltwater flow through the differing refreezing capacity of the snowpack and therefore can lead to different melt features in firn. The profiles above show extreme examples of (a) cold firn with distinct melt layers, lenses and vertical flow fingers, and (b) temperate snow characterized by more homogeneous progression of the melting front and wide-spread grain coarsening. A continuum between these extremes allows for unique site- and event-specific structural manifestations of melt events under natural conditions.

Further investigation of commonalities and differences among melt features will facilitate the development of a standardised description and identification scheme for melt-affected ice cores. This includes a more detailed structural description of melt layers in ice cores from various climates including their natural variability, how to handle the interplay of melt and firn, or how to interpret thicker melt layers seemingly resulting from several events.

3.2 Melt-affected chemical proxy records

Melting has diverse effects on ice-core records of, e.g., major ions, trace elements, organic compounds, or BC. Depending on the chemical species, study site, and amount of melting, anything between a drastic disturbance and fully preserved records has been reported in literature. For example, NH_4^+ (Avak et al., 2019; Trachsel et al., 2019), BC (Festi et al., 2021; Osmont et al., 2018; Pavlova et al., 2015), ^3H (Pinglot et al., 2003), low-abundant water-soluble and insoluble trace elements (Wong et al., 2013) appear to be rather preserved. On the other hand, melt-induced alteration is a substantial issue for H_2O_2 (Moser et al., 2021), major ions like SO_4^{2-} and Ca^{2+} (Eichler et al., 2001; Li et al., 2006; Virkkunen et al., 2007) and high-abundant water-soluble trace elements (Avak et al., 2018, 2019).

Chemical impurities in the snow/firn part of a glacier can be, to varying degree, eluted from their original position of deposition and enriched either in a deeper layer during refreezing or in the meltwater run-off. Whether impurity species are displaced

410 within or lost from a profile depends on the refreezing capacity of the subsurface, which can be anything between predominantly cold firn to generally temperate snow and firn. Elution has been a research topic since the 1970s, because it leads to an environmentally relevant 'ion flush' from snowpacks at the start of the melt season (Costa & Pomeroy, 2019; Johannessen et al., 1977; Johannessen & Henriksen, 1978; Tsiouris et al., 1985). In this context, 'preferential elution' of certain ions compared to others has been observed, and a multitude of elution sequences for major ions has been published (Table 1

415 and references therein).

Table 1: Chronological overview of studies on elution behaviour and sequences of major ions conducted in the field and laboratory using firn and ice-core sections, snow and meltwater composition measurements, and elution experiments. Elution sequences show strongly affected species left and more stable impurities to the right. The position of sulfate (bright pink), calcium (purple), chloride
420 **(dark blue) and ammonium (light blue) are highlighted in the elution sequences. Note that different study conditions and presentation of elution in the referenced literature complicate a direct comparison.**

Study Type	Location	Study	Publication Year	Elution Sequence
including firn and ice cores	Folgefonna, Norway	Davies et al.	1982	SO_4^{2-}, $Mg^{2+} > NO_3^- > Na^+$, $Cl^- > NH_4^+$, K^+
	18 C, Greenland	Goto-Azuma et al.	1994	$NO_3^- > SO_4^{2-} > Cl^-$
	Ürümqi Glacier No.1, Tian Shan	Goto-Azuma et al.	1994	$NO_3^- > Mg^{2+} > SO_4^{2-}$, $Na^+ > Ca^{2+}$, $Cl^- > K^+$
	Austre Brøggerbreen, Svalbard	Goto-Azuma et al.	1994	NO_3^-, $SO_4^{2-} > Na^+$, Cl^-
	Upper Grenzgletscher, Switzerland	Eichler et al.	2001	$SO_4^{2-} > Ca^{2+}$, $Mg^{2+} > K^+$, $Na^+ >> NO_3^- > NH_4^+$, $F^- > Cl^-$
	Lomonosovfonna, Svalbard	Moore et al.	2005	$NO_3^- > SO_4^{2-} > Ca^{2+}$, MSA^-, $K^+ > Cl^- > Na^+$, $NH_4^+ > Mg^{2+}$
	Lomonosovfonna, Svalbard	Virkkunen et al.	2007	SO_4^{2-}, Ca^{2+}, Mg^{2+}, $NO_3^- > K^+ > Cl^- > Na^+ > NH_4^+$
	Nevado Coropuna Saddle, Peru	Herreros et al.	2009	$SO_4^{2-} > NO_3^- > Mg^{2+} > NH_4^+ > Ca^{2+} > Na^+ > K^+ > Cl^- > Br-$
	Lomonosovfonna snow pit, Svalbard	Moore & Grinsted	2009	Ca^{2+}, SO_4^{2-}, Mg^{2+}, $NO_3^- > K^+ > Cl^- > Na^+ > NH_4^+$
	Lomonosovfonna ice core, Svalbard	Moore & Grinsted	2009	SO_4^{2-}, $NO_3^- > Mg^{2+} > Ca^{2+} > Cl^- > Na^+ > K^+ > NH_4^+$
	Austre Brøggerbreen, Svalbard	Moore & Grinsted	2009	$Mg^{2+} > SO_4^{2-} > NO_3^- > Ca^{2+} > Cl^- > Na^+ > K^+ > NH_4^+$
	Chimborazo, Ecuador	Ginot et al.	2010	$SO_4^{2-} > Ca^{2+} > Mg^{2+} > F^- > Na^+$, $K^+ > Cl^- > NO_3^- > NH_4^+$, $HCOO^-$
	Lomonosovfonna, Svalbard	Vega et al.	2016	$NO_3^- > SO_4^{2-} > Mg^{2+}$, Cl^-, K^+, Na^+
	Grand Combin, Switzerland	Huber et al.	2020	$MSA^- > SO_4^{2-}$, $C_2O_4^-$, $Ca^{2+} > NO_3^-$, $Mg^{2+} > F^-$, NH_4^+
Measurements of snow and/or meltwater	Cairn Gorm Mountain, Scotland	Brimblecombe et al.	1985	$SO_4^{2-} > NO_3^- > NH_4^+ > K^+ > Ca^{2+} > Mg^{2+} > H^+ > Na^+ > Cl^-$
	Ürümqi Glacier No.1, Tian Shan	Li et al.	2006	$SO_4^{2-} > Ca^{2+} > Na^+ > NO_3^- > Cl^- > K^+ > Mg^{2+} > NH_4^+$
	Holtedahlfonna, Spitsbergen	Virkkunen et al.	2007	SO_4^{2-}, Ca^{2+}, Mg^{2+}, $NO_3^- > K^+ > Cl^- > Na^+ > NH_4^+$
	Baishui Glacier No.1, Tibetian Plateau	Pang et al.	2012	$NO_3^- > SO_4^{2-} > K^+ > Cl^- > Mg^{2+} > Ca^{2+} > Na^+$ (profile 1)
	Baishui Glacier No.1, Tibetian Plateau	Pang et al.	2012	$K^+ > SO_4^{2-} > NO_3^- > Cl^- > Ca^{2+} > Mg^{2+} > Na^+$ (profile 2)
	Midtre Lovénbreen, Svalbard	Björkman et al.	2014	SO_4^{2-}, $Cl^- > NO_3^-$, Na^+, $K^+ > Mg^{2+} > Ca^{2+} > F^-$, $NH_4^+ >$ microbes
	Ürümqi Glacier No.1, Tian Shan	You et al.	2015	$SO_4^{2-} >> Mg^{2+}$
	Shiyi Glacier, Qilian Mountains	Zong-Xing et al.	2015	$SO_4^{2-} > K^+ > Ca^{2+} > Mg^{2+} > Na^+ > Cl^- > NO_3^-$
	Lomonosovfonna, Svalbard	Vega et al.	2016	$NO_3^- > SO_4^{2-} > Mg^{2+}$, Cl^-, K^+, Na^+

	Tapado Glacier, Chile	Sinclair & MacDonell	2016	SO_4^{2-}, Na^+, Mg^{2+}, Ca^{2+} >> Cl^-
	Ürümqi Glacier No.1, Tian Shan	Wu et al.	2018	Ca^{2+} > Na^+ > Mg^{2+} > K^+
	Baishui Glacier No.1, Tibetian Plateau	Wang et al.	2018	Ca^{2+} > SO_4^{2-} > NH_4^+ > K^+ > NO_3^- > Na^+ > Cl^- > Mg^{2+}
	Weißfluhjoch, Switzerland	Avak et al.	2019	SO_4^{2-}, Ca^{2+}, NO_3^- > Na^+, Cl^- > NH_4^+
	Weißfluhjoch, Switzerland	Trachsel et al.	2019	Ca^{2+}, SO_4^{2-}, Na^+ > NH_4^+, F^-, Cl^-
	Austre Brøggerbreen, Svalbard	Spolaor et al.	2021	Na^+ > I^- > Br^- > K^+ > Mg^{2+} > Ca^{2+} > Cl^- (melt events)
	Austre Brøggerbreen, Svalbard	Spolaor et al.	2021	Mg^{2+} > Na^+ > K^+ > SO_4^{2-} > Ca^{2+} > I^- > Cl^- > MSA^- (rain on snow)
Elution experiments	Southeastern Norway	Johannessen et al.	1977	SO_4^{2-} > Ca^{2+} > Mg^{2+} > H^+ > NH_4^+ > Cl^- > NO_3^- > Na^+ > K^+
	Folgefonna, Norway	Tsiouris et al.	1985	Ca^{2+} > NO_3^- > K^+ > Mg^{2+} > SO_4^{2-} > Na^+ > Cl^-
	—	Hewitt et al.	1989	SO_4^{2-} > Ca^{2+}, Mg^{2+} > K^+ > Na^+ > NO_3^- > Cl^-
	—	Tranter et al.	1992	SO_4^{2-} > Mg^{2+} > Na^+, NO_3^- > Cl^-
	Sasagamine, Niigata, Japan	Goto-Azuma et al.	1993	NO_3^- > SO_4^{2-} > Cl^-
	—	Herrmann & Kranz	1995	Alkali metals, alkaline earth metals, cations (other than NH_4^+) > SO_4^{2-} > NO_3^- > Cl^- > NH_4^+ > H_2O_2
	—	Cragin et al.	1996	SO_4^{2-}, NO_3^- > … > Cl^-
	—	Costa & Pomeroy	2019	PO_4^{3-} > NO_3^- > Cl^- > SO_4^{2-} > F^-
Review	—	Kuhn	2001	SO_4^{2-} > NO_3^- > Cl^-
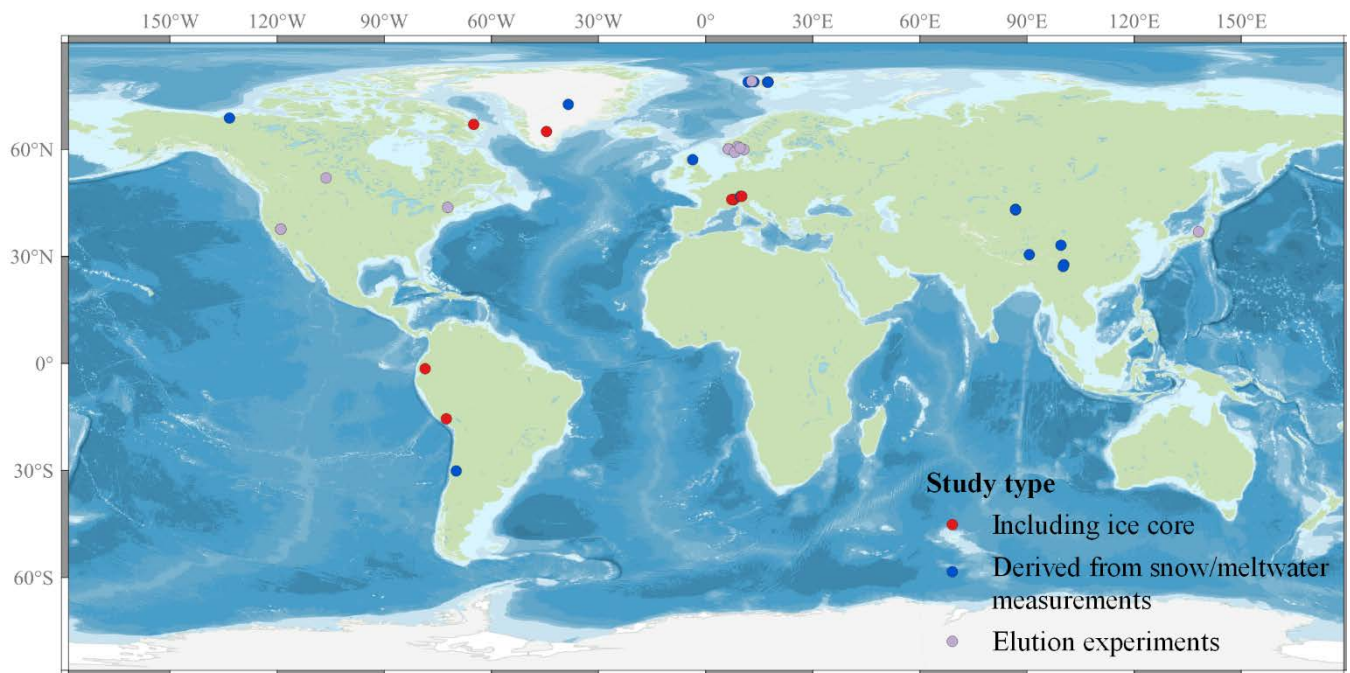
Figure 4: Overview of study sites, where the effects of melting on major ion chemistry has been conducted using ice cores (red), snow and meltwater measurements in the field (blue) and elution experiments in the laboratory and field (light purple).

425

The elution sequences presented in Table 1 have been obtained from natural and synthetic snow and ice samples, in field and laboratory experiments, e.g. lysimeter measurements, at various sites as well as from modelling approaches (Fig. 4). Related to the different sites and study conditions, and to the sample material of varying age and composition, there is partial

430   disagreement in the exact position of ions in the sequence. Nevertheless, sulfate and calcium tend to be among the ions eluted more quickly, while fluoride, chloride and ammonium appear more stable (Table 1, Fig. 5). Since snow has been shown to reveal no chromatographic properties, this is not due to a potential retention of latter species in the snow/firn with respect to former ones during elution (Cragin et al., 1996; Hewitt et al., 1989; Tranter et al., 1986). Instead, several other factors shaping the elution sequences of different major ions and also other chemical species have been identified.

435
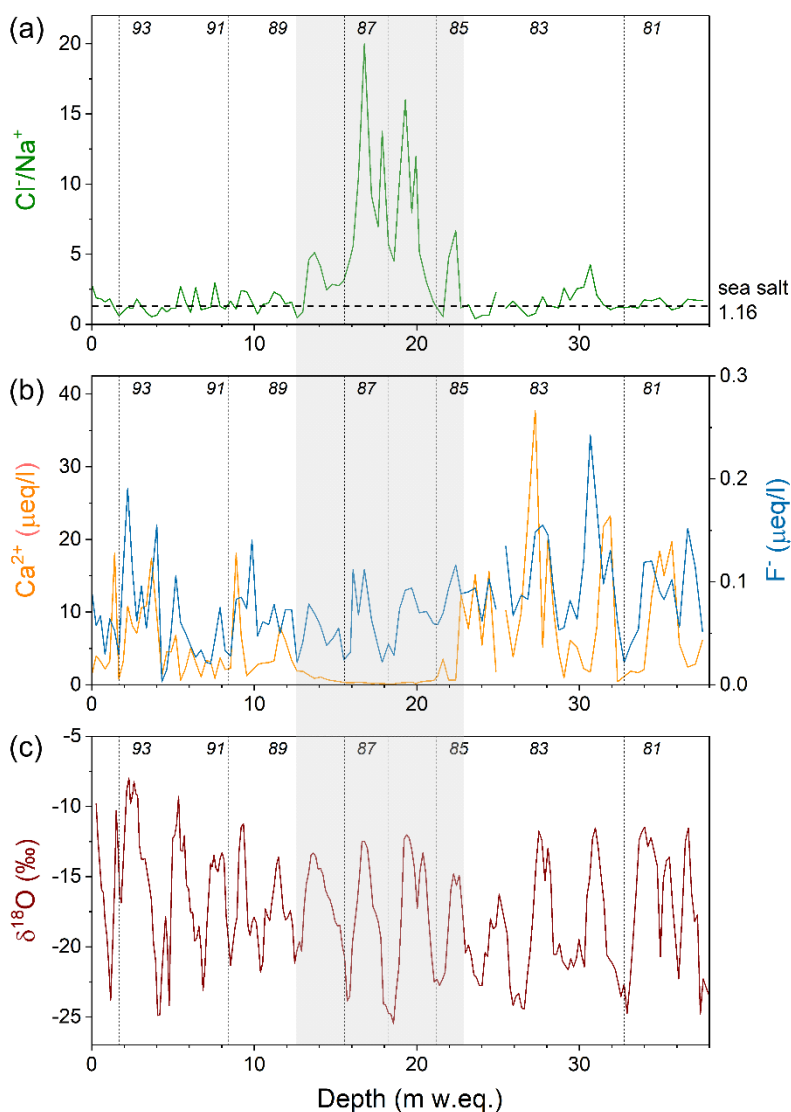
Figure 5: Records of Cl⁻/Na⁺ ratio (green), Ca²⁺ (orange) and F⁻ (blue) concentrations, and δ¹⁸O (brown) within the upper 38 m w.eq. of an ice core from Grenzgletscher (Swiss Alps, Eichler et al., 2001), covering the time period 1980–1994 (individual years are indicated, dotted lines): Meltwater inflow through a crevasse system led to (a) high Cl⁻/Na⁺ ratios, exceeding the sea-salt ratio (1.16, dashed line) in the melt-disturbed range (grey background), (b) preferential elution of Ca²⁺ compared to F⁻, with the latter still showing well-preserved concentration seasonality in the depth range ~12–23 m w.eq., (c) whereas δ¹⁸O is mainly undisturbed; observations suggest lack of refreezing of the percolating meltwater but drainage along the firn-ice transition.

The primary determining factor for the behaviour of impurities during elution is their solubility in water (Meyer & Wania, 2011; Fig. 6) and ice (Avak et al., 2019). A high solubility in ice, e.g. observed for F⁻, Cl⁻, NH₄⁺, allows for chemical species to be incorporated into the ice lattice during snow metamorphism and thereby reduces their availability to meltwater elution (Cragin et al., 1996; Trachsel et al., 2019; Eichler et al., 2001), while high solubility in water enhances their mobility during melt events. Insoluble microparticles are less affected by displacement to deeper layers of the snowpack and can show melt-induced peaks at former surfaces (Koerner, 1977b, 1997). Meyer and Wania (2011) have modelled the elution behaviour of organic compounds from a homogeneous snowpack and distinguish four elution types (Fig. 6): (a) impurities strongly soluble in water are released quickly after melt onset; (b) particulate matter and surface-adsorbed impurities elute last; (c) meltwater concentrations of species that are partly water-soluble and partly sorbed to ice grain surfaces increase gradually with melt duration; (d) bimodal impurities that can behave both like dissolved type (a) and particulate type (b) show peak concentrations at the beginning and end of the snowmelt season.
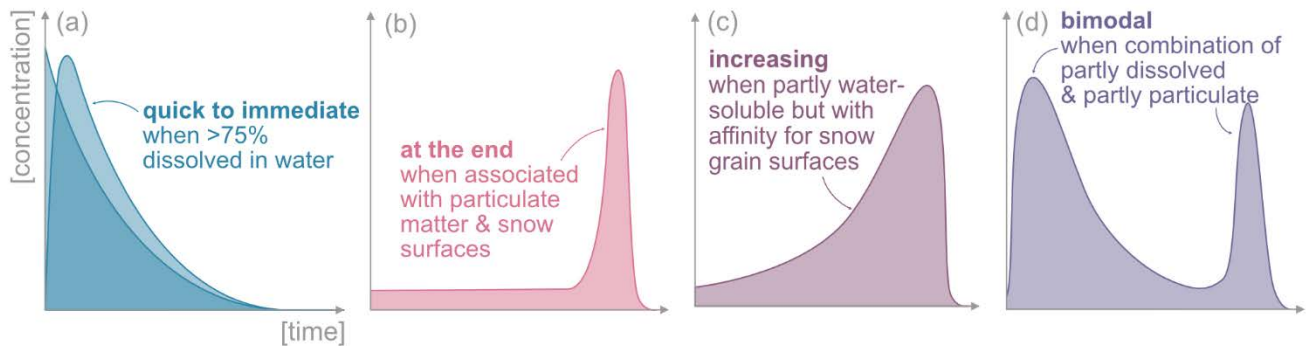
Figure 6: Differences in behaviour during melt elution of (a) water-soluble impurities, (b) particle-bound matter, (c) species that are partly water-soluble and partly sorbed to ice grain surfaces, and (d) impurities combining the dissolved type (a) and particulate type (b); this is a schematic summary based on modelling of organic compounds during melt by Meyer and Wania (2011).

Besides their solubility in water and ice, (1) snow characteristics prior to melting, (2) snow metamorphism, and (3) the character of the melt process itself can subordinately influence the elution behaviour of impurities (Fig. 7).

(1) Initially, precipitation formation or atmospheric scavenging processes influence the chemical composition of the snow and its absolute ion concentrations and thus, the impurity behaviour during elution. The initial position of impurities within the ice-air matrix depends on whether they act as condensation nuclei during snow crystal formation (placed within crystal) or are scavenged and found in the exterior of snow grains (Trachsel et al., 2019; Tsiouris et al., 1985). However, even ions that have been deposited together like Na^+ and Cl^- (sea-salt aerosol) showed partially different behaviour during leaching (Eichler et al., 2001), and metamorphism subdues this factor post-depositionally. Since only a certain amount of impurities can be incorporated into the ice lattice, absolute concentrations affect the number of ions placed at grain boundaries, where they are more available to interaction with meltwater (Fig. 7: right (1)). Less abundant (partially) water-soluble trace elements appear to be more stable than the ones with higher absolute concentrations (Avak et al., 2018, 2019; Li et al., 2006).

(2) The physical location of impurities within the ice matrix is relevant beyond the initial position and undergoes changes with ageing during snow metamorphism (Fig. 7: right (2); Kuhn, 2001; Moore et al., 2005; Pohjola et al., 2002; Trachsel et al., 2019; Tsiouris et al., 1985). Earlier studies suggest that diurnal melt-freeze cycles generally enhance the availability of ions to leaching during percolation (Johannessen and Henriksen, 1978; Goto-Azuma et al., 1994). However, it has been shown that rearrangement behaviour during metamorphism differs among impurities (Cragin et al., 1996; Hewitt et al., 1989; Trachsel et al., 2019) mainly depending on their solubility in ice (Avak et al., 2019; Eichler et al., 2001). For ions, this solubility in ice is influenced by their size and charge (Moore & Grinsted, 2009) but also by the capability to form volatile compounds, which is e.g. significant for Cl^-, F^-, NO_3^-, and NH_4^+ (Eichler et al., 2001; Li et al., 2006). On this basis, Cl^-, NH_4^+ and F^- tend to be incorporated in the ice matrix during advancing metamorphism (Eichler et al., 2001; Ginot et al., 2010; Moore et al., 2005; Trachsel et al., 2019), whereas SO_4^{2-} and Ca^{2+} tend to be excluded and are more readily available to meltwater relocation. The effect of metamorphism on the preservation or loss of ions in the snowpack becomes increasingly apparent with longer duration of metamorphism (Brimblecombe et al., 1987; Cragin et al., 1996; Trachsel et al., 2019).

Furthermore, the temperature-gradient metamorphism conditions, especially absolute (diurnal mean) air temperatures and their diurnal variability (Li et al., 2006; Virkkunen et al., 2007), determine between constructive and deconstructive metamorphism, influence the near-surface snow grain shape, and indirectly constrain the availability of impurities at grain boundaries through the snow surface area (Fig. 7: right (2)). Constructive metamorphism leads to hoar and faceted crystals with a higher specific surface area and the solubility-driven separation between interior and exterior of a snow grain is less effective than during deconstructive metamorphism in rounded grains (Cragin et al., 1996). A temperature gradient is generally necessary to achieve recrystallisation rates that lead to significant chemical re-arrangement (Trachsel et al., 2019).

(3) Differences in meltwater flow type, melt rate, addition of rain on snow, and snow structure make the character of the melt event itself a shaping factor for elution behaviour of ions (Fig. 7: right (3)). Costa and Pomeroy (2019) documented that preferential flow paths speed up the release of SO_4^{2-} and NO_3^- from the snowpack. A slower melt rate leads to higher ionic pulses (Davis et al., 1995), because it allows for longer interaction with and leaching of the snow. Similarly, melt events without rain on snow appear to be more efficient in eluting SO_4^{2-} and NO_3^-, because PFPs developing under these circumstances result from microscale flow structures (Costa & Pomeroy, 2019; Tranter et al., 1992) that differ from hydrologically constrained PFPs during rain-on-snow events. Furthermore, the snow texture (e.g. specific surface area, SSA) strongly affects hydrological permeability, and less or im-/permeable layers can lead to the retaining and refreezing of ion-enriched meltwater within the profile (Pfeffer & Humphrey, 1996).
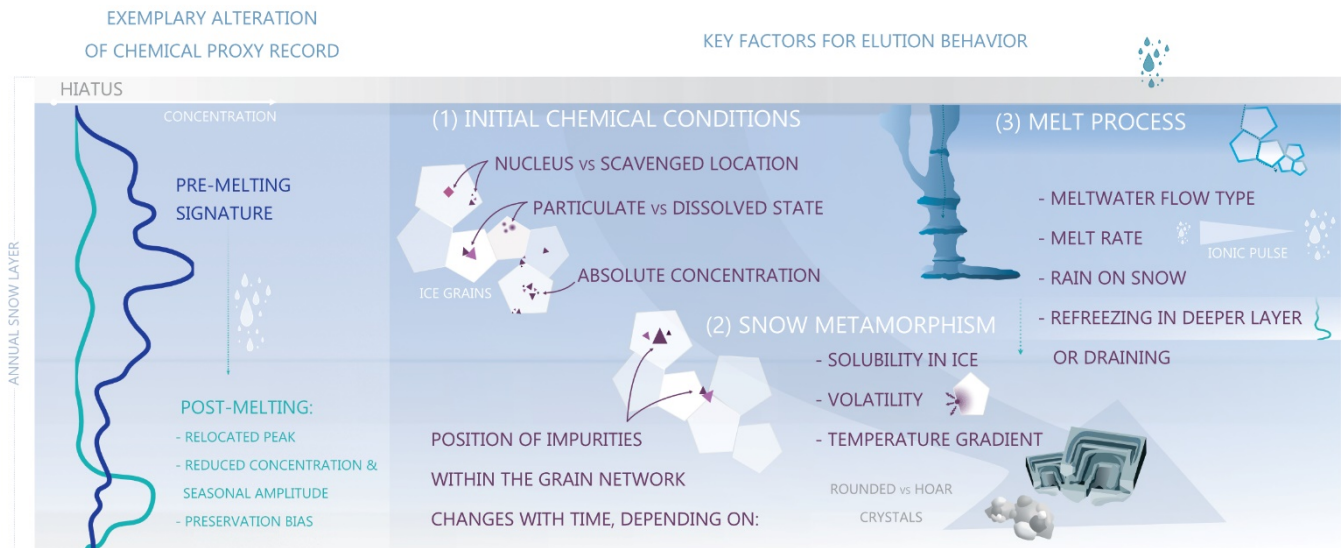
Figure 7: Schematic display of issues associated with melt-affected ice-core chemistry using a qualitative drawing (left), and key factors for elution behaviour of impurities (right) include (1) initial chemical conditions of the deposited snow, (2) segregation of impurities during snow metamorphism, and (3) the melt process itself.

Melt-induced alteration of chemical ice-core proxy records have further been assessed using ion elution factors (Moore & Grinsted, 2009), ion ratios like Mg^{2+}/Na^+ (Iizuka et al., 2002; Watanabe et al., 2015) and Cl^-/Na^+ (e.g. Fig. 5, Eichler et al., 2001), and based on the dissolved fraction percentage (DFP, Wu et al., 2018; Zhang et al., 2013). Comparing concentrations of a chemical species in a snow layer before and after a melt event is the basis of elution factor quantification (Moore & Grinsted, 2009). The ion ratio approaches indicate melt-affected profile sections based on the differing elution factor of two ions like Mg^{2+} and Na^+, which have a common source at the investigated site. The DFP is defined as:

$$DFP = X_{dis} / (X_{dis}+X_{insol}) \times 100\%$$
(Eq. 3)

520

Changes in the preserved ions-to-microparticles ratio of soluble (X_{dis}) and insoluble fraction (X_{insol}) as formulated in Equation 3 reflect the intensity of post-depositional alteration through melting when source and composition of the impurities are homogeneous in a layer prior to melting (Zhang et al., 2013). When compared against DFP values of non-melt affected parts from the same site, lowered DFP signatures reflect the mobility of dissolved and immobility of insoluble impurities during

525   elution (Fig. 6; Fig. 7). Therefore, site-specific influences on the behaviour of chemical species used for Mg^{2+}/Na^+, Cl^-/Na^+ ion ratios and DFP must be considered. While elution factor and Mg^{2+}/Na^+ or Cl^-/Na^+ ratio calculations are easier in their application, the DFP has the advantage that it can identify gradual stages of elution.

Finally, the questions remain, to which extent and in which way climate and environmental information are still preserved in

530   melt-affected chemical records. Firstly, dating melt-affected ice cores has proven challenging in locations ranging from alpine (Festi et al., 2021; Pavlova et al., 2015) through to sub-Antarctic sites like Young Island (Moser et al., 2021). In this context, the melt-induced hiatus in the ice-core layering during melt events (Koerner, 1997) is a major issue. If sufficient summer precipitation is altered or removed (Yuanqing et al., 2001), it can lead to a seasonal bias of the net annual layer towards winter accumulation. In addition, the resolution in melt-affected chemical records can be lowered from seasonal to (multi-)annual

535   (Moore & Grinsted, 2009; Vega et al., 2016) due to a reduction of soluble ion concentrations and of the amplitudes of seasonal proxies like hydrogen peroxide (Davies et al., 1982; Huber et al., 2020; Moser et al., 2021). Consequently, annual layer counting as a dating approach can be severely hampered in melt-affected soluble impurity records. However, using chemical species less affected by meltwater percolation such as NH_4^+, insoluble trace elements and particulate records like BC has already proven valuable for dating melt-affected ice (Avak et al., 2019; Neff et al., 2012; Pavlova et al., 2015). With regard to

540   more confined dating horizons, ^{137}Cs cannot be used due to its melt-induced relocation, but [3]H (Pinglot et al., 2003; Van Der Wel et al., 2011) and [210]Pb (Gäggeler et al., 2020; Neff et al., 2012) remain viable as dating tools.

Both (1) percolation extent and (2) species-dependent elution behaviour must be considered in order to decide which melt-affected chemical impurity records can still be used for environmental reconstructions, and how they can be used.

545   (1) Elution length determines the preserved resolution of melt-affected chemical impurity records. Annual means of environmental proxies remain suitable where melt is seasonally confined. For example, this is the case at Lomonosovfonna in Svalbard (Moore et al., 2005; Pohjola et al., 2002; Vega et al., 2016), Penny Ice Cap (Grumet et al., 1998) and Combatant Col at Mount Waddington in Canada (Neff et al., 2012). If percolation affects more than one annual layer, multi-year averages are more reliable, e.g. at Severnaya Zemlya in the Eurasian Arctic (Weiler et

550   al., 2005), Holtedahlfonna (Beaudon et al., 2013), or Austfonna in Svalbard (Tarussov, 1992).

(2) Among major ions, vertical concentration profiles of NH_4^+, F^- and Cl^- are generally better preserved than those of Ca^{2+}, SO_4^{2-} (Table 1). Thus, NH_4^+ is preferred to SO_4^{2-} for reconstructing anthropogenic changes, and Cl^- preferred to Na^+ for investigating sea-salt changes. For trace elements (TEs), it has been shown that insoluble, particle-bound TEs

are rather immobile (Avak et al., 2018, 2019; Gabrieli et al., 2011; Wong et al., 2013), whereas relocation of water-soluble TEs depends on their absolute concentration levels, with ultra-TEs better preserved. Thus, past changes in dust input can be established more reliably using rare earth elements (REEs) instead of Ba, Mg or Ca records. Pb, Cu, Sb, and Ag are still applicable for anthropogenic reconstructions, whereas Cd and Zn are less reliable proxies. Looking at organic species, the few available studies show widely differing responses to meltwater input depending on whether the organic material consists of dissolved, hydrophobic or adsorbed species (Meyer & Wania, 2011; Schöndorf & Herrmann, 1987; Simmleit et al., 1986). For example, polychlorinated biphenyls lean towards relocation (Pavlova et al., 2015), and out of selected mono- and dicarboxylic acids and α-carbonyls, only methylglyoxal showed potential as a better-preserved organic aerosol proxy in melt-affected records (Müller-Tautges et al., 2016). Regarding particulate impurities like BC (and pollen), preserved annual cycles in temperate glaciers suggest that BC and pollen can still provide an important environmental proxy even under strong melting conditions (Festi et al., 2021; Pavlova et al., 2015; Takeuchi et al., 2019). Consequently, BC appears to be more suitable, e.g., for reconstructing the forest-fire history compared to organic fire proxies prone to leaching such as *P*-hydroxybenzoic acid (Müller-Tautges et al., 2016).

It must be noted that the observed meltwater persistence of certain species at one location is not directly transferrable to ice-core archives from other sites (e.g. Table 1). Since the impurity response to post-depositional melting processes is shaped by numerous factors like impurity concentrations, chemical composition, mineralogy, or amount of meltwater, it may vary between remote and polluted regions, different climate conditions, or with the distance to deserts and oceans. Thus, the preservation of chemical species, in each case, requires site-specific assessment.

3.3 Stable water isotopic (SWI) signatures affected by melt

Isotopic fractionation is fundamental to the interpretation of stable water isotopes (SWI, Gat, 1996) as climate proxies in ice cores, and an extensive body of ice-core scientific literature starting with the pioneering work by Dansgaard (1964) exists on this topic. Here, we solely discuss alterations of SWI through melting and refreezing, because the fractionation of heavier and lighter isotopes takes place during phase changes, so that melting and refreezing in the snowpack plays a significant role (Koerner et al., 1973). Due to isotopic exchange between liquid water and surrounding ice matrix, the linear slope between the abundance of $\delta^{18}O$ and $\delta^{2}H$ is considered altered (Ham et al., 2019; Lee et al., 2020). While normally displaying a slope of 8, it is often lowered in melt-affected ice (Souchez & Jouzel, 1984). For this reason, melt-affected SWI signatures have been considered biased (Koerner et al., 1973; Moran & Marshall, 2009), i.e. enriched in heavy isotopes ^{18}O and ^{2}H. The presence of liquid water further leads to smoothing of the stable water isotopic records in snow pits and ice cores (Kang et al., 2008; Matsuoka & Naruse, 1999; Nye, 1998), "with the degree of smoothing dependent on the amount of melting and percolation" (Arnason et al., 1973; Pohjola et al., 2002). Another effect of percolation frequently discussed is the redistribution of isotopic signatures into deeper layers, which causes the mixing of signatures from different seasons (Koerner, 1997; Fig.7). Both altered

fractionation and signal percolation can lead to an amplitude reduction or entire loss of the seasonal cycle preserved in stable water isotope ratios like $\delta^{18}O$ (Moran & Marshall, 2009; Rempel et al., 2001; Shiraiwa et al., 2002; Yuanqing et al., 2001).

590 The preservation of deposited isotopic signatures depends on the interplay of various factors and remains a subject of research. If percolation is mainly pore flow and leaves the ice matrix intact, for example when the liquid-ice contact time is short, the SWI signal is less affected. Percolation depth is another important factor for $\delta^{18}O$ preservation, as melting and refreezing limited to the surface leads to distinct ice layers (Sect. 2.2 & 3.1), which can act as impermeable barriers for diffusion caused by movement of water vapour (Van Der Wel et al., 2011). The study argues that ice cores affected by short-term melt and 595 refreezing events, which divide the snow column into separate pore spaces, could exhibit more reliable stable water isotope records, because water vapour diffusion between the spaces is prohibited.

Several studies from SWI records at melt-affected sites proved to reliably record past temperature changes with seasonal resolution, e.g. in the Swiss Alps (Eichler et al., 2001; Fig. 5) and Patagonia (Schwikowski et al., 2013), or at annual resolution, 600 e.g. in Canada (Neff et al., 2012), Svalbard (Pohjola et al., 2002; Van Der Wel et al., 2011), and Siberian Altai (Okamoto et al., 2011). Where percolation is not restricted to annual layers, multi-year averages could still be used. For example, long-term (>5 years) climate variability is currently still preserved at Holtedahlfonna, Svalbard, despite seasonal variability being lost (Spolaor et al., 2023). When considering millennial-scale features, the $\delta^{18}O$ ratios in a melt-affected part of the North Greenland Eemian Ice Drilling ('NEEM') ice core seem unaffected (NEEM community members, 2013). On the contrary, at Quelccaya 605 Ice Cap in Peru, strong meltwater-related smoothing of the annual signal and an increase of the SWI ratios between two cores drilled in 1976 and 1991 has been observed, rendering the reconstruction of past temperature from SWI ratios impossible at this site (Thompson et al., 1993). Similarly severe smoothing issues and loss of $\delta^{18}O$ as dating tool and climate proxy have been reported at Hielo Patagónico Norte, South America (Matsuoka & Naruse, 1999), and numerous other low-latitude high-altitude glaciers (Thompson et al., 2021, and references therein). The recent study by Spolaor et al. (2023) highlights how 610 intensifying melt has gradually degraded the SWI records from Holtedahlfonna, Svalbard, over the course of less than a decade. Thus, the reliability of SWI records from melt-affected ice cores as climate proxies is strongly dependent on the study site and progressing melt conditions.

3.4 Gas records affected by melt

Atmospheric air entering the snow at the surface is diffusing through the snow and firn reaching the bottom of the firn column 615 much faster than snow of the same age. In the so-called lock-in-zone, the pore space within the firn closes off, thereby trapping the air at 50–100 m below the snow surface depending on local conditions (Neff, 2014). This leads to an absolute age difference between ice and gas phase commonly referred to as delta age (Δage; Schwander & Stauffer, 1984), which depends on the vertical compaction of the firn column, mainly a function of snow accumulation at the surface, and can range from decades

for higher accumulation sites to many millennia for the East Antarctic plateau (Bazin et al., 2013; Buizert et al., 2015; Roberts
620 et al., 2017; Veres et al., 2013).

In contrast to the chemical parameters discussed in Sect. 3.3, samples of atmospheric air trapped in tiny bubbles in the ice matrix are only indirectly affected by melt. The influence of melt layers in the firn column on the movement of air and bubble enclosure characteristics remains poorly understood (Keegan et al., 2014, 2019; Trudinger et al., 1997). Assuming that melt

625 layers behave similar to (very) dense layers of firn, published research on gas diffusion in non-melt affected firn suggests:

(1) Discontinuous melt layers may act as a vertical barrier and enhance horizontal air flow, thereby potentially reducing the effects of gravitational settling (Birner et al., 2018; Craig et al., 1988). However, in non-extreme cases melt lenses likely cannot completely prohibit air diffusion.

(2) Frequent melt layers may leave a lasting effect on firn metamorphism (Keegan et al., 2019) potentially changing the

630 pore volume and increasing the height of the lock-in-zone. The latter would cause younger air to be trapped earlier, leading to a decrease in the mean age of the trapped air, i.e. it may widen the gas age distribution in closed bubbles (Mitchell et al., 2015).

Focussing on the gases contained, melt layers differ from non-melt-affected ice found below the lock-in zone in three important

635 ways. Most importantly, air is dissolved in the meltwater following Henry's law. Depending on the speed of refreezing, not all of these gases will degas, and some fraction will remain trapped in the refrozen melt feature. The relative amount fractions of key gas species used for palaeoclimatic reconstructions, including carbon dioxide (CO_2), methane (CH_4), and noble gases Argon (Ar), Krypton (Kr) and Xenon (Xe), increase by differing amounts relative to the atmospheric levels in liquid water (Ahn et al., 2008; Neftel et al., 1983; Orsi et al., 2015). In a melt layer, the CO_2 amount fraction may increase by up to two

640 orders of magnitude relative to the atmospheric amount fraction with equilibrium levels at ≥16,000 ppm at 0°C (Ahn et al., 2008; Weiss, 1974), so even trace amounts of melt have the potential to significantly alter atmospheric CO_2 reconstructions. Note that over centuries to many millennia, the gas trapped in the melt layer will slowly diffuse into the surrounding layers of firn/ice driven by a large concentration gradient and alter the composition of trapped air once the melt layer passed the lock-in zone, thereby also altering the gas composition in the surrounding ice on the cm-scale (Ahn et al., 2008). The same issue of

645 gas dissolution is encountered during wet extraction commonly used for CH_4 amount fraction measurements and requires a dissolution correction, while the dry-extraction or sublimation methods typically used for CO_2 measurements prevents this as no water is present in these cases. The absolute gas concentrations in melt-affected profiles depend on (1) the speed at which melt is refreezing, (2) gas equilibration while passing through the firn column, and (3) the amount of atmospheric air trapped in the melt-layers during bubble enclosure (Stauffer et al., 1985).

650

Secondly, the presence of liquid water may trigger the production of CO_2, CH_4 and nitrous oxide (N_2O) of non-atmospheric origin in the ice, either by acid-carbonate reaction (Ahn et al., 2008; Delmas, 1993; Orsi et al., 2015; Tschumi & Stauffer,

2000), oxidation or biodegradation of organic compounds (Lee et al., 2020; Tschumi & Stauffer, 2000), or microbial production (Lee et al., 2020; NEEM community members, 2013). Together with the solubility-related increase of greenhouse

655 gases, amount fractions as high as 2000 ppm CO_2 (Ahn et al., 2008; Neftel et al., 1983), 1200 ppb CH_4, and 150 ppb N_2O (NEEM community members, 2013) above background levels for Greenlandic ice cores have been reported. The production potential for Antarctic ice core is much lower due to overall lower dust deposition, but still sufficient to significantly alter the atmospheric amount fractions (Ahn et al., 2008).

660 Lastly, total air content (TAC) is often interpreted as driven by, among other effects, the elevation of the glacier surface, i.e. higher elevation is associated with lower TAC as the barometric air pressure decreases with altitude (Delmotte et al., 1999; Martinerie et al., 1992). However, a reduced TAC may also be indirectly caused by a melt feature because the presence of impermeable ice, i.e. the refrozen melt layer, has replaced porous firn and thereby lowered the volume of pore space in melt-affected firn in the lock-in zone. This may lead up to 40% reduction in TAC (Stauffer et al., 1985), even though this reduction

665 does not seem to be consistent throughout different melt features and ice cores. TAC within a melt layer likely depends on the speed at which the meltwater refreezes, with faster rates being associated with higher TAC due to less time available for degassing of the gas solved in the water phase (Ahn et al., 2008; NEEM community members, 2013; Orsi et al., 2015). Observations from the Greenland NEEM ice core during the Eemian Interglacial show that TAC varies more strongly during warm phases with more frequent melt events (NEEM community members, 2013).

670

The effects described above can be used to identify and quantify depth sections affected by melt. While the presence of a melt layer may lead to a major increase in greenhouse gas amount fractions, excessive amounts of greenhouse gases alone are not sufficient to identify melt, because of the potential for in-situ production in the absence of liquid water (Schilt et al., 2010; Tschumi & Stauffer, 2000). Noble gases, on the other hand, are not produced in-situ. The solubility of the noble gases Kr and

675 Xe are approximately two and four times greater than for Ar, which has proven to be a sensitive tool to confirm suspected melt in deep sections of the Greenland NEEM ice core (Orsi et al., 2015). Orsi et al. (2015) showed that $\delta(Kr/Ar)$ and $\delta(Xe/Ar)$ of melt-affected depth sections, 44±12‰ and 109±34‰ (n=6), were significantly higher than background levels of unaffected ice, 13±2‰ and 24 ±4‰. Based on only two samples, Ahn et al. (2008) reported even greater sensitives for $\delta(Kr/Ar)$ and $\delta(Xe/Ar)$ of melt-affected section in excess of 100‰ and 250‰, respectively. If the presence of even small amounts of melt

680 is suspected, a pre-emptive scan of the ice for hidden melt is a sensitive tool. Unfortunately, the necessity for preparing discrete samples, large ice sample requirements (typically 2–3x 50–60 g), and a limited daily sample throughput of the noble gas method (Orsi et al., 2015) do not allow for a systematic implementation. It should be noted that the noble gas method cannot quantify the melt intensity.

Aside from noble gases, low TAC could be interpreted as an indicator for melt, as has been suggested based on TAC simulation

685 (Plach et al., 2021; Vudayagiri et al., 2018). However, this method requires evidence of a significant TAC decrease for visible

melt layers for the studied ice core, and the TAC for melt layers may be very similar to non-melt affected ice (Orsi et al., 2015).

So far, only two lower-elevation Antarctic ice cores with small amounts of melt have been used for gas reconstructions. Firstly,
690   the Law Dome ice core, which was drilled on an isolated dome at 1370 m above sea level close to the continental edge of East
Antarctica and contains ≤5 melt layers (Etheridge et al., 1996; Trudinger et al., 1997). Secondly, the Siple Dome ice core, which is located on the West Antarctic Ice Sheet at an altitude of 620 m and shows numerous melt layers (Ahn et al., 2004; Ahn & Brook, 2014; Das & Alley, 2005). Visible melt layers have been avoided during sampling for gas reconstructions for both ice cores. According to Ahn et al. (2004), it can further not be excluded that the observed absolute offsets between CO_2
695   measurements from Siple Dome relative to EPICA Dome C may stem from in-situ production.
Though melt layers are less rare in Greenland (Alley & Anandakrishnan, 1995; Chappellaz et al., 1997; NEEM community members, 2013; Neftel et al., 1983), ice cores from central Greenland have been used for gas reconstructions (Blunier & Brook, 2001; Schilt et al., 2010). In such high-altitude ice cores, the occurrence of melt features is likely limited to the Holocene and Last Interglacial warm periods, and records covering the Last Glacial are affected to a lesser extent. However, CO_2
700   reconstructions from Greenland are considered unreliable due to significant in-situ production of non-atmospheric CO_2, which takes place in the ice sheet over time even in the absence of liquid water (Tschumi & Stauffer, 2000).

3.5 Current applications of melt layers as proxies

The primary application of melt layers in ice cores is as qualitative and quantitative temperature proxy (Alley & Anandakrishnan, 1995; Kameda et al., 1995; Okamoto et al., 2011). It is based on the non-linear relationship between
705   frequency and thickness of melt features and temperatures above freezing and has led to melt-temperature records from alpine to polar sites (Abram et al., 2013; Das & Alley, 2008; Fujita et al., 2019). Comparisons between melt layer and $\delta^{18}O$ records (Grumet et al., 2001; Henderson et al., 2006; Koerner et al., 1973), nearby weather stations and reanalysis data (Fujita et al., 2019) have been used to show the coherence of derived temperature records. Thereby, it has been noted that the occurrence of melt features depicts complex dynamics at any ice-core site (Alley & Anandakrishnan, 1995). While melt is assumed to reflect
710   summer temperature conditions rather than annual mean temperature (Herron et al., 1981; Koerner, 1977a; Koerner & Fisher, 1990), the relevance of winter melt events is not to be underestimated for alpine to coastal polar sites (Zheng et al., 2020), especially since winter temperatures are rising more quickly than summer temperatures at mid-latitude and Arctic sites (Graham et al., 2017). An increasing number of melt layers can be caused (a) by an absolute temperature rise during one or several seasons of the year, (b) enhanced variability of temperatures during at least one season, or (c) a combination of both
715   (Das & Alley, 2008). Changes of external parameters like elevation of ice cap surfaces can also affect the local climate and melt conditions (Das & Alley, 2008; Fig. 2). Furthermore, the near- and sub-surface firn conditions affect the prominence of melt features, with melt layers appearing more distinctly in cold firn than in homogeneously wetted, temperate firn (see

Sect. 2.2 & 3.1.). All factors discussed in Sect. 2 affect the frequency and thickness of melt features and are helpful context for quantitatively interpreting melt layer profiles. Against this background, certain sites and glacier facies like the lower accumulation zone, where melting occurs but doesn't percolate through the entire annual layer, are more sensitive to the melt threshold and therefore more suitable sites for melt records than others (Abram et al., 2013). Given the uncertainty induced by percolation, Westhoff et al. (2022) have cautioned against the interpretation of melt layer profiles as annually resolved temperature proxy records and recommended ≥10-year averages. Using the dependency of melt occurrence on warm temperatures, Okamoto et al. (2011) have also been able to show that melt feature percentage correlates with terminus retreat rate of a neighbouring glacier.

Besides the simple occurrence of melt layers, significant potential lies in the structural characteristics of melt features as proxy for environmental conditions. Based on the physics of melt layer formation, structural characteristics of melt features are expected to differ dependent of meteorological setting and local climate, which leave an imprint on the near-surface snow (Fig. 3). Early studies have shown that warm summers were characterized by coarser-grained superimposed ice than colder summers with fine-grained firn (Koerner, 1970; Koerner et al., 1973). Future studies of melt-affected ice cores could describe the structural variability of melt features in ice cores in greater detail and thereby provide new insights into the processes shaping melt features.

Another emerging research area comes from the relationship between forest fires, consequential BC dust distribution and enhanced glacier melt (Kaspari et al., 2015; Keegan et al., 2014). Given that BC is a reliable tracer of forest fires even in melt-affected areas (Osmont et al., 2020), comparing BC and melt feature records could reveal new aspects for interpreting melt features as proxies.

4 Conclusions and outlook

Global temperature is rising and melting will affect a growing number of alpine to polar ice-core drilling locations, more frequently, at higher elevation, and further inland. For this reason, we have conducted a literature review, bringing together snow physics, firn hydrology and ice-core proxy research, for studying melt-affected ice cores.

Melt events are driven by local to global meteorology and climate, glacier surface characteristics like the albedo, and hydro-thermal conditions of the snow and firn column. Melting and refreezing is governed by the surplus of energy available and follows approximately the 0°C isotherm. Identification of melt layers usually takes place either manually during ice-core processing, discriminating between melt-affected and unaffected firn sections, or using digital line scanning, which provides higher-resolution insights into melt characteristics. Approaches like this show the diverse structural imprints of snowmelt on the ice-air matrix, ranging from homogeneously wetted horizons to distinct melt layers and preferential flow fingers. Those develop depending on the dynamic interplay of atmosphere and subsurface conditions and hold potential as environmental proxy.

Preferential elution is the primary issue of melt-affected ice-core chemistry. Dominated by solubility of the impurities in water and ice, a multitude of factors, including snow chemistry before melting, metamorphism and meltwater flow conditions, determines the availability of impurities to relocation or removal during melt events. Thus, the preservation of chemical species strongly differs with the study site. Where significant amounts of liquid water are present, the fractionation slope for stable water isotopes (δ^2H/ δ^{18}O) is reduced and affected records often show an amplitude reduction of the seasonal cycle, biased values and smoothing of the signal. Altered total air content and gas concentrations must be considered for melt-affected gas records in ice cores.

Despite these limitations of melt-affected ice cores, melt layers have been successfully applied as qualitative (above 0°C) and quantitative temperature proxy (using MFP as an indicator of surface temperature). Approaches ranging from using ion ratios (e.g. Mg^{2+}/Na^+) and the dissolved fraction percentage in the upper ice column to noble gases Xenon and Krypton in deep ice help to identify the extent of ice profiles affected by melting and refreezing.

Our literature study shows that melting poses both challenges and potential for ice-core interpretation and dating approaches, and also that the diversity of melt features and effects are of interest for comprehensive and site-specific investigation. Learning from the advances of alpine ice-core science, the following adaptations have been shown to be helpful to ensure high-quality ice-core research under warming conditions.

1. (Re-)assessing the thermal and hydrological conditions of the subsurface prior to drilling helps to target ice-core analysis to predominantly cold, poly-thermal or temperate ice.

2. Sampling fresh (near-)surface snow throughout the seasonal cycle allows to establish a baseline of impurity levels prior to melting, and in-situ snowmelt infiltration experiments using dye can be used to parametrize relocation depth site-specifically.

3. High-resolution structural analysis of ice cores (e.g. line scanning), more detailed melt logs including feature characteristics, and systematic assessments of melt indicators (e.g. DFP, Cl^-/Na^+ ion ratio) provide useful context to better understand chemical records.

4. Prioritization of impurities less mobile during melt events like ammonium, BC, insoluble and low-abundant (partially) water-soluble trace elements as dating tools and environmental proxies, and using multi-year averages where melt percolates beyond an annual layer leads to more reliable environmental reconstructions.

With this review we contribute to a growing body of literature aiming to foster a comprehensive understanding of signal formation in ice cores and to improve their climatic interpretations. We hope to raise awareness among (polar) ice-core researchers about melt features in ice cores, how to identify and investigate them in greater detail, and how to gauge limitations and potential of melt-affected profiles for ice-core climate reconstructions.

Author contributions. DEM and ERT conceptualized the study. DEM organised the project and conducted the literature analysis fundamental to this study. ERT and EW supervised the project. DEM prepared the initial draft, and all co-authors contributed to review and editing of the manuscript including figures.

Competing interests. The authors declare that they have no conflict of interest.

785 *Funding.* DEM was supported by BAS Cambridge, and the NERC C-CLEAR Doctoral Training Programme (grant no.NE/S007164/1). ERT received core funding from NERC to the British Antarctic Survey's Ice Dynamics and Palaeoclimate programme. EW is supported by a Royal Society Professorship.

Acknowledgments. The authors want to thank Margit Schwikowski, who was consulted and provided experienced external advice for Sect. 3.2 on melt-affected chemistry records. The authors also would like to acknowledge the editorial support from
790 Kerim Nisancioglu and thank Veijo Pohjola and an anonymous reviewer for their valuable suggestions. The melt layer images used in Fig. 1a and Fig. 1i have been reprinted from the Journal of Glaciology, and the melt layer image in Fig. 1f has been reprinted from the Annals of Glaciology with permission of the International Glaciological Society. The image used in Fig. 1d is reprinted from Global and Planetary Change Volumes 84–85, Fisher et al., Recent melt rates of Canadian arctic ice caps are the highest in four millennia, 3–7 (2012), with permission from Elsevier. The melt layer sequence in Fig. 1h is reprinted from
795 Nature Geoscience Volume 6, Abram et al., Acceleration of snow melt in an Antarctic Peninsula ice core during the twentieth century, 404–411 (2013), with permission from Springer Nature.

References.

800 Abram, N. J., Mulvaney, R., Wolff, E. W., Triest, J., Kipfstuhl, S., Trusel, L. D., Vimeux, F., Fleet, L., & Arrowsmith, C. (2013). Acceleration of snow melt in an Antarctic Peninsula ice core during the twentieth century. *Nature Geoscience*, *6*, 404–411. https://doi.org/10.1038/ngeo1787

Ahn, J., & Brook, E. J. (2014). Siple Dome ice reveals two modes of millennial CO_2 change during the last ice age. *Nature Communications*, *5*, 1–6. https://doi.org/10.1038/ncomms4723

805 Ahn, J., Headly, M., Wahlen, M., Brook, E. J., & Mayewski, P. A. (2008). CO(2) Diffusion in Polar Ice: Observations from Naturally Formed CO(2) Spikes in the Siple Dome (Antarctica) Ice Core. *Earth Science Faculty Scholarship*, *24*. https://digitalcommons.library.umaine.edu/ers_facpub/24

Ahn, J., Wahlen, M., Deck, B. L., Brook, E. J., Mayewski, P. A., Taylor, K. C., & White, J. W. C. (2004). A record of atmospheric CO_2 during the last 40,000 years from the Siple Dome, Antarctica ice core. *Journal of Geophysical*
810 *Research D: Atmospheres*, *109*(13), 1–8. https://doi.org/10.1029/2003JD004415

Albert, M., Shuman, C., Courville, Z., Bauer, R., Fahnestock, M., & Scambos, T. (2004). Extreme firn metamorphism: impact of decades of vapor transport on near-surface firn at a low-accumulation glazed site on the East Antarctic plateau. *Annals of Glaciology*, *39*, 73–78. https://doi.org/10.3189/172756404781814041

Alimasi, N., Enomoto, H., & Hirasawa, N. (2020). Spatiotemporal variation of ice sheet melting in the Antarctic coastal marginal zone and the influence of ice lenses and rain using satellite microwave observation. *Polar Science*, *25*(July), 100561. https://doi.org/10.1016/j.polar.2020.100561

Alley, R. B., & Anandakrishnan, S. (1995). Variations in melt-layer frequency in the GISP2 ice core: implications for Holocene summer temperatures in central Greenland. *Annals of Glaciology*.

Arnason, B., Buason, T., Martinec, J., & Theodorsson, P. (1973). Movement of water through snow pack traced by deuterium and tritium. *IAHS Publication*, *107*, 299–312.

Arnold, N. S., Rees, W. G., Hodson, A. J., & Kohler, J. (2006). Topographic controls on the surface energy balance of a high Arctic valley glacier. *Journal of Geophysical Research: Earth Surface*, *111*(2), 1–15. https://doi.org/10.1029/2005JF000426

Avak, S. E., Schwikowski, M., & Eichler, A. (2018). Impact and implications of meltwater percolation on trace element records observed in a high-Alpine ice core. *Journal of Glaciology*, *64*(248), 877–886. https://doi.org/10.1017/jog.2018.74

Avak, S. E., Trachsel, J. C., Edebeli, J., Brütsch, S., Bartels-Rausch, T., Schneebeli, M., Schwikowski, M., & Eichler, A. (2019). Melt-Induced Fractionation of Major Ions and Trace Elements in an Alpine Snowpack. *Journal of Geophysical Research: Earth Surface*, *124*(7), 1647–1657. https://doi.org/10.1029/2019JF005026

Avanzi, F., Hirashima, H., Yamaguchi, S., Katsushima, T., & De Michele, C. (2016). Observations of capillary barriers and preferential flow in layered snow during cold laboratory experiments. *Cryosphere*, *10*(5), 2013–2026. https://doi.org/10.5194/tc-10-2013-2016

Banwell, A. F., Tri Datta, R., Dell, R. L., Moussavi, M., Brucker, L., Picard, G., Shuman, C. A., & Stevens, L. A. (2021). The 32-year record-high surface melt in 2019/2020 on the northern George VI Ice Shelf, Antarctic Peninsula. *Cryosphere*, *15*(2), 909–925. https://doi.org/10.5194/tc-15-909-2021

Bazin, L., Landais, A., Lemieux-Dudon, B., Toyé Mahamadou Kele, H., Veres, D., Parrenin, F., Martinerie, P., Ritz, C., Capron, E., Lipenkov, V., Loutre, M. F., Raynaud, D., Vinther, B., Svensson, A., Rasmussen, S. O., Severi, M., Blunier, T., Leuenberger, M., Fischer, H., … Wolff, E. (2013). An optimized multi-proxy, multi-site Antarctic ice and gas orbital chronology (AICC2012): 120-800 ka. *Climate of the Past*, *9*(4), 1715–1731. https://doi.org/10.5194/cp-9-1715-2013

Beaudon, E., Moore, J. C., Martma, T., Pohjola, V. A., Van De Wal, R. S. W., Kohler, J., & Isaksson, E. (2013). Lomonosovfonna and Holtedahlfonna ice cores reveal east-west disparities of the Spitsbergen environment since AD 1700. *Journal of Glaciology*, *59*(218), 1069–1083. https://doi.org/10.3189/2013JoG12J203

Bell, R. E., Banwell, A. F., Trusel, L. D., & Kingslake, J. (2018). Antarctic surface hydrology and impacts on ice-sheet mass balance. *Nature Climate Change*, *8*(12), 1044–1052. https://doi.org/10.1038/s41558-018-0326-3

Bell, R. E., Chu, W., Kingslake, J., Das, I., Tedesco, M., Tinto, K. J., Zappa, C. J., Frezzotti, M., Boghosian, A., & Lee, W. S. (2017). Antarctic ice shelf potentially stabilized by export of meltwater in surface river. *Nature*, *544*(7650), 344–348. https://doi.org/10.1038/nature22048

Birner, B., Buizert, C., Wagner, T. J. W., & Severinghaus, J. P. (2018). The influence of layering and barometric pumping on firn air transport in a 2-D model. *Cryosphere*, *12*(6), 2021–2037. https://doi.org/10.5194/tc-12-2021-2018

Bishop, C. L., Pan, D., Liu, L. M., Tribello, G. A., Michaelides, A., Wang, E. G., & Slater, B. (2009). On thin ice: surface order and disorder during pre-melting. *Faraday Discussions*, *141*(0), 277–292. https://doi.org/10.1039/B807377P

Björkman, M., Zarsky, J., Kühnel, R., Hodson, A., Sattler, B., & Psenner, R. (2014). Microbial Cell Retention in a Melting High Arctic Snowpack, Svalbard. *Arctic, Antarctic, and Alpine Research*, *46*(2), 471–482. https://doi.org/10.1657/1938-4246-46.2.471

Blunier, T., & Brook, E. J. (2001). Timing of Millennial-Scale Climate Change in Antarctica and Greenland During the Last Glacial Period. *Science*, *291*(5501), 109–112. https://doi.org/10.1126/science.291.5501.109

Box, J. E., Wehrlé, A., van As, D., Fausto, R. S., Kjeldsen, K. K., Dachauer, A., Ahlstrøm, A. P., & Picard, G. (2022). Greenland Ice Sheet Rainfall, Heat and Albedo Feedback Impacts From the Mid-August 2021 Atmospheric River. *Geophysical Research Letters*, *49*(11). https://doi.org/10.1029/2021GL097356

Brimblecombe, P., Clegg, S. L., Davies, T. D., Shooter, D., & Tranter~, M. (1987). Observations of the preferential loss of major ions from melting snow and laboratory ice. *Water Research*, *21*(10), 1279–1286. https://doi.org/10.1016/0043-1354(87)90181-3

Brown, J. W., Moser, D. E., Emanuelsson, D. B., & Thomas, E. R. (2023). Visual Stratigraphy-Based Age Scale Developed for the Shallow Mount Siple Firn Core, Antarctica. *Geosciences*, *13*(3), 85. https://doi.org/10.3390/geosciences13030085

Brun, E. (1989). Investigation on wet-snow metamorphism in respect of liquid-water content. *Annals of Glaciology*, *13*, 22–26. https://doi.org/10.3189/S0260305500007576

Buizert, C., Cuffey, K. M., Severinghaus, J. P., Baggenstos, D., Fudge, T. J., Steig, E. J., Markle, B. R., Winstrup, M., Rhodes, R. H., Brook, E. J., Sowers, T. A., Clow, G. D., Cheng, H., Edwards, R. L., Sigl, M., McConnell, J. R., & Taylor, K. C. (2015). The WAIS Divide deep ice core WD2014 chronology – Part 1: Methane synchronization (68-31 ka BP) and the gas age-ice age difference. *Climate of the Past*, *11*(2), 153–173. https://doi.org/10.5194/cp-11-153-2015

Campbell, F. M. A., Nienow, P. W., & Purves, R. S. (2006). Role of the supraglacial snowpack in mediating meltwater delivery to the glacier system as inferred from dye tracer investigations. *Hydrological Processes*, *20*(4), 969–985. https://doi.org/10.1002/hyp.6115

Cape, M. R., Vernet, M., Skvarca, P., Marinsek, S., Scambos, T., & Domack, E. (2015). Foehn winds link climate-driven warming to ice shelf evolution in Antarctica. *Journal of Geophysical Research*, *120*(21), 11,037-11,057. https://doi.org/10.1002/2015JD023465

Chappellaz, J., Brook, E., Blunier, T., & Malaizé, B. (1997). CH4 and δ18O of O2 records from Antarctic and Greenland ice: A clue for stratigraphic disturbance in the bottom part of the Greenland Ice Core Project and the Greenland Ice Sheet Project 2 ice cores. *Journal of Geophysical Research: Oceans*, *102*(C12), 26547–26557. https://doi.org/10.1029/97JC00164

Clem, K. R., Fogt, R. L., Turner, J., Lintner, B. R., Marshall, G. J., Miller, J. R., & Renwick, J. A. (2020). Record warming at the South Pole during the past three decades. *Nature Climate Change*, *10*(8), 762–770. https://doi.org/10.1038/s41558-020-0815-z

Clerx, N., Machguth, H., Tedstone, A., Jullien, N., Wever, N., Weingartner, R., & Roessler, O. (2022). In situ measurements of meltwater flow through snow and firn in the accumulation zone of the SW Greenland Ice Sheet. *EGUsphere [Preprint]*. https://doi.org/10.5194/egusphere-2022-71

Colbeck, S. C. (1982). An Overview of Seasonal Snow Metamorphism. *Reviews of Geophysics and Space Sciences*, *20*(1), 45–61. https://doi.org/10.1029/RG020i001p00045

Conway, H., Gades, A., & Raymond, C. F. (1996). Albedo of dirty snow during conditions of melt. *Water Resources Research*, *32*(6), 1713–1718.

Costa, D., & Pomeroy, J. W. (2019). Preferential meltwater flowpaths as a driver of preferential elution of chemicals from melting snowpacks. *Science of the Total Environment*, *662*(January), 110–120. https://doi.org/10.1016/j.scitotenv.2019.01.091

Cragin, J. H., Hewitt, A. D., & Colbeck, S. C. (1996). Grain-scale mechanisms influencing the elution of ions from snow. *Atmospheric Environment*, *30*(1), 119–127. https://doi.org/10.1016/1352-2310(95)00232-N

Craig, H., Horibe, Y., & Sowers, T. (1988). Gravitational Separation of Gases and Isotopes in Polar Ice Caps. *Science*, *242*(4886), 1675–1678. http://www.jstor.org/stable/1703399

Cuffey, K., & Paterson, W. S. B. (2010). *The Physics of Glaciers* (4th ed.). Academic Press.

Culberg, R., Schroeder, D. M., & Chu, W. (2021). Extreme melt season ice layers reduce firn permeability across Greenland. *Nature Communications*, *12*(2336), 1–9. https://doi.org/10.1038/s41467-021-22656-5

Cullather, R. I., & Nowicki, S. M. J. (2018). Greenland Ice Sheet surface melt and its relation to daily atmospheric conditions. *Journal of Climate*, *31*(5), 1897–1919. https://doi.org/10.1175/JCLI-D-17-0447.1

Dansgaard, W. (1964). Stable isotopes in precipitation. *Tellus*, *16*(4), 436–468. https://doi.org/10.3402/tellusa.v16i4.8993

Das, S. B., & Alley, R. B. (2005). Characterization and formation of melt layers in polar snow: observations and experiments from West Antarctica. *Journal of Glaciology*, *51*(173), 307–312. https://doi.org/10.3189/172756505781829395

Das, S. B., & Alley, R. B. (2008). Rise in frequency of surface melting at Siple Dome through the Holocene: Evidence for increasing marine influence on the climate of West Antarctica. *Journal of Geophysical Research Atmospheres*, *113*(2), 1–11. https://doi.org/10.1029/2007JD008790

Datta, R. T., Tedesco, M., Fettweis, X., Agosta, C., Lhermitte, S., Lenaerts, J. T. M., & Wever, N. (2019). The Effect of Foehn-Induced Surface Melt on Firn Evolution Over the Northeast Antarctic Peninsula. *Geophysical Research Letters*, *46*(7), 3822–3831. https://doi.org/10.1029/2018GL080845

Davies, T., Vincent, C., & Brimblecombe, P. (1982). Preferential elution of strong acids from a Norwegian ice cap. *Nature*, *300*, 161–163. https://doi.org/10.1038/300161a0

Davis, R. E., Petersen, C. E., & Bales, R. C. (1995). Ion flux through a shallow snowpack: effects of initial conditions and melt sequences. *IAHS Publications*, *228*, 115.

Dell, R. L., Banwell, A. F., Willis, I. C., Arnold, N. S., Halberstadt, A. R. W., Chudley, T. R., & Pritchard, H. D. (2021). Supervised classification of slush and ponded water on Antarctic ice shelves using Landsat 8 imagery. *Journal of Glaciology*, 1–14. https://doi.org/10.1017/jog.2021.114

Delmas, R. J. (1993). A natural artefact in Greenland ice-core CO2 measurements. *Tellus, Series B*, *45 B*(4), 391–396. https://doi.org/10.3402/tellusb.v45i4.15737

Delmotte, M., Raynaud, D., Morgan, V., & Jouzel, J. (1999). Climatic and glaciological information inferred from air-content measurements of a Law Dome (East Antarctica) ice core. *Journal of Glaciology*, *45*(150), 255–263. https://doi.org/10.3189/S0022143000001751

Dey, R., Thamban, M., Laluraj, C. M., Mahalinganathan, K., Redkar, B. L., Kumar, S., & Matsuoka, K. (2022). Application of visual stratigraphy from line-scan images to constrain chronology and melt features of a firn core from coastal Antarctica. *Journal of Glaciology*, 1–12. https://doi.org/DOI: 10.1017/jog.2022.59

Dirmhirn, I., & Eaton, F. (1975). Some Characteristics of the Albedo of Snow. *Journal of Applied Meteorology and Climatology*, *14*(3), 375–379. https://doi.org/10.1175/1520-0450(1975)014<0375:SCOTAO>2.0.CO;2

Eichler, A., Schwikowski, M., & Gäggeler, H. W. (2001). Meltwater-induced relocation of chemical species in Alpine firn. *Tellus, Series B: Chemical and Physical Meteorology*, *53*(2), 192–203. https://doi.org/10.3402/tellusb.v53i2.16575

Elvidge, A. D., & Renfrew, I. A. (2016). The Causes of Foehn Warming in the Lee of Mountains. *Bulletin of the American Meteorological Society*, *97*(3), 455–466. https://doi.org/10.1175/BAMS-D-14-00194.1

EPICA Community Members. (2004). Eight glacial cycles from an Antarctic ice core. *Nature*, *429*, 623–628. https://doi.org/10.1038/nature02599

Etheridge, D. M., Steele, L. P., Langenfelds, R. L., Francey, R. J., Barnola, J. M., & Morgan, V. I. (1996). Natural and anthropogenic changes in atmospheric CO2 over the last 1000 years from air in Antarctic ice and firn. *Journal Of Geophysical Research-Atmospheres*, *101*(D2), 4115–4128. https://doi.org/10.1029/95JD03410

Faraday. (1859). On regelation, and on the conservation of force. *The London, Edinburgh, and Dublin Philosophical Magazine and Journal of Science*, *17*(113), 162–169. https://doi.org/10.1080/14786445908642645

Fegyveresi, J. M., Alley, R. B., Muto, A., Orsi, A. J., & Spencer, M. K. (2018). Surface formation, preservation, and history of low-porosity crusts at the WAIS Divide site, West Antarctica. *Cryosphere*, *12*(1), 325–341. https://doi.org/10.5194/tc-12-325-2018

Festi, D., Schwikowski, M., Maggi, V., Oeggl, K., & Jenk, T. M. (2021). Significant mass loss in the accumulation area of the Adamello glacier indicated by the chronology of a 46m ice core. *Cryosphere*, *15*(8), 4135–4143. https://doi.org/10.5194/tc-15-4135-2021

Fisher, D., Zheng, J., Burgess, D., Zdanowicz, C., Kinnard, C., Sharp, M., & Bourgeois, J. (2012). Recent melt rates of Canadian arctic ice caps are the highest in four millennia. *Global and Planetary Change*, *84–85*, 3–7. https://doi.org/10.1016/j.gloplacha.2011.06.005

Fountain, A. G., Tranter, M., Nylen, T. H., Lewis, K. J., & Mueller, D. R. (2004). Evolution of cryoconite holes and their contribution to meltwater runoff from glaciers in the McMurdo Dry Valleys, Antarctica. *Journal of Glaciology*, *50*(168), 35–45. https://doi.org/10.3189/172756504781830312

Frezzotti, M., Gandolfi, S., & Urbini, S. (2002). Snow megadunes in Antarctica: Sedimentary structure and genesis. *Journal of Geophysical Research Atmospheres*, *107*(18). https://doi.org/10.1029/2001JD000673

Fricker, H. A., Arndt, P., Brunt, K. M., Datta, R. T., Fair, Z., Jasinski, M. F., Kingslake, J., Magruder, L. A., Moussavi, M., Pope, A., Spergel, J. J., Stoll, J. D., & Wouters, B. (2021). ICESat-2 Meltwater Depth Estimates: Application to Surface Melt on Amery Ice Shelf, East Antarctica. *Geophysical Research Letters*, *48*(8). https://doi.org/10.1029/2020GL090550

Fritzsche, D., Schütt, R., Meyer, H., Miller, H., Wilhelms, F., Opel, T., & Savatyugin, L. M. (2005). A 275 year ice-core record from Akademii Nauk ice cap, Severnaya Zemlya, Russian Arctic. *Annals of Glaciology*, *42*, 361–366. https://doi.org/DOI: 10.3189/172756405781812862

Fujita, K., Matoba, S., Iizuka, Y., Takeuchi, N., & Aoki, T. (2019). Physically based summer temperature reconstruction from ice layers in ice cores. *Climate of The Past Discussions*, 1–28. https://doi.org/10.5194/cp-2019-97

Gabrieli, J., Carturan, L., Gabrielli, P., Kehrwald, N., Turetta, C., Cozzi, G., Spolaor, A., Dinale, R., Staffler, H., Seppi, R., Dalla Fontana, G., Thompson, L., & Barbante, C. (2011). Impact of Po Valley emissions on the highest glacier of the Eastern European Alps. *Atmospheric Chemistry and Physics*, *11*(15), 8087–8102. https://doi.org/10.5194/acp-11-8087-2011

Gäggeler, H. W., Tobler, L., Schwikowski, M., & Jenk, T. M. (2020). Application of the radionuclide 210Pb in glaciology-an overview. *Journal of Glaciology*, *66*(257), 447–456. https://doi.org/10.1017/jog.2020.19

Gat, J. R. (1996). Oxygen and Hydrogen Isotopes in the Hydrological Cycle. *Annual Review of Earth and Planetary Sciences*, *24*(1), 225–262. https://doi.org/10.1146/annurev.earth.24.1.225

Gilbert, E., & Kittel, C. (2021). Surface Melt and Runoff on Antarctic Ice Shelves at 1.5°C, 2°C, and 4°C of Future Warming. *Geophysical Research Letters*, *48*(8). https://doi.org/10.1029/2020GL091733

Ginot, P., Chappellaz, J., Barbante, C., Schwikowski, M., & Ohlmann, A.-C. (2021). Ice Memory. *EGU General Assembly Conference Abstracts*, EGU21-8842.

Ginot, P., Schotterer, U., Stichler, W., Godoi, M. A., Francou, B., & Schwikowski, M. (2010). Influence of the Tungurahua eruption on the ice core records of Chimborazo, Ecuador. *Cryosphere*, *4*(4), 561–568. https://doi.org/10.5194/tc-4-561-2010

Goto-Azuma, K., Nakawo, M., Jiankang, H., & Watanabe, O. (1994). Melt-induced relocation of ions in glaciers and in a seasonal snowpack. *Publication of the International Association of Hydrologial Sciences*, *223*(423), 287–297.

Goto-Azuma, K., Nakawo, M., Shimizu, M., Azuma, N., Nakayama, M., & Yokoyama, K. (1993). Temporal changes in chemical stratigraphy of snow cover. *Annals of Glaciology*, *18*, 85–91. https://doi.org/10.3189/s0260305500011307

Graeter, K. A., Osterberg, E. C., Ferris, D. G., Hawley, R. L., Marshall, H. P., Lewis, G., Meehan, T., McCarthy, F., Overly, T., & Birkel, S. D. (2018). Ice Core Records of West Greenland Melt and Climate Forcing. *Geophysical Research Letters*, *45*(7), 3164–3172. https://doi.org/10.1002/2017GL076641

Graham, R. M., Cohen, L., Petty, A. A., Boisvert, L. N., Rinke, A., Hudson, S. R., Nicolaus, M., & Granskog, M. A. (2017). Increasing frequency and duration of Arctic winter warming events. *Geophysical Research Letters*, *44*(13), 6974–6983. https://doi.org/https://doi.org/10.1002/2017GL073395

Grumet, N. S., Wake, C. P., Mayewski, P. A., Zielinski, G. A., Whitlow, S. I., Koerner, R. M., Fisher, D. A., & Woollett, J. M. (2001). Variability of Sea-Ice Extent in Baffin Bay over the Last Millennium. *Climatic Change*, *49*, 129–145. https://doi.org/10.1023/A:1010794528219

Grumet, N. S., Wake, C. P., Zielinski, G. A., Fisher, D., Koerner, R., & Jacobs, J. D. (1998). Preservation of glaciochemical time-series in snow and ice from the Penny Ice Cap, Baffin Island. *Geophysical Research Letters*, *25*(3), 357–360. https://doi.org/10.1029/97GL03787

Hahn, L. C., Hofer, S., Parfitt, R., & Ummenhofer, C. C. (2020). Importance of Orography for Greenland Cloud and Melt Response to Atmospheric Blocking. *Journal of Climate*, *33*(10), 4187–4206. https://doi.org/10.1175/JCLI-D-19-0527.1

Ham, J. Y., Hur, S. Do, Lee, W. S., Han, Y., Jung, H., & Lee, J. (2019). Isotopic variations of meltwater from ice by isotopic exchange between liquid water and ice. *Journal of Glaciology*, *65*(254), 1035–1043. https://doi.org/10.1017/jog.2019.75

Hanna, E., Fettweis, X., Mernild, S. H., Cappelen, J., Ribergaard, M. H., Shuman, C. A., Steffen, K., Wood, L., & Mote, T. L. (2014). Atmospheric and oceanic climate forcing of the exceptional Greenland ice sheet surface melt in summer 2012. *International Journal of Climatology*, *34*(4), 1022–1037. https://doi.org/10.1002/joc.3743

Hanna, E., Jones, J. M., Cappelen, J., Mernild, S. H., Wood, L., Steffen, K., & Huybrechts, P. (2013). The influence of North Atlantic atmospheric and oceanic forcing effects on 1900-2010 Greenland summer climate and ice melt/runoff. *International Journal of Climatology*, *33*(4), 862–880. https://doi.org/10.1002/joc.3475

Heggli, M., Köchle, B., Matzl, M., Pinzer, B. R., Riche, F., Steiner, S., Steinfeld, D., & Schneebeli, M. (2011). Measuring snow in 3-D using X-ray tomography: Assessment of visualization techniques. *Annals of Glaciology*, *52*(58), 231–236. https://doi.org/10.3189/172756411797252202

Henderson, K., Laube, A., Gäggeler, H. W., Olivier, S., Papina, T., & Schwikowski, M. (2006). Temporal variations of accumulation and temperature during the past two centuries from Belukha ice core, Siberian Altai. *Journal of Geophysical Research Atmospheres*, *111*(3). https://doi.org/10.1029/2005JD005819

Herreros, J., Moreno, I., Taupin, J.-D., Ginot, P., Patris, N., De Angelis, M., Ledru, M.-P., Delachaux, F., & Schotterer, U. (2009). Environmental records from temperate glacier ice on Nevado Coropuna saddle, southern Peru. *Adv. Geosci*, *22*, 27–34. https://doi.org/10.5194/adgeo-22-27-2009

Herrmann, R., & Kranz, J. (1995). Release of Major Ions and Hydrogen Peroxide from Homogeneous, Melting Snow. *Nordic Hydrology*, *26*, 359–368.

Herron, M., Herron, S., & Langway, C. (1981). Climatic signal of ice melt features in southern Greenland. *Krueger, A. 1. & Minzer, R. A. J. Geophys. Res*, *293*(9), 389–391. https://doi.org/10.1038/293389a0

Herron, M. M., & Langway, C. C. (1980). Firn densification: an empirical model. *Journal of Glaciology*, *25*(93), 373–385. https://doi.org/10.3189/S002214300001523

Hewitt, A. D., Cragin, J. H., & Colbeck, S. C. (1989). Does Snow Have Chromatographic Properties? *Proceedings of the 46th Annual Eastern Snow Conference*, 165–171.

Hirashima, H., Avanzi, F., & Wever, N. (2019). Wet-Snow Metamorphism Drives the Transition From Preferential to Matrix Flow in Snow. *Geophysical Research Letters*, *46*(24), 14548–14557. https://doi.org/10.1029/2019GL084152

Hirashima, H., Avanzi, F., & Yamaguchi, S. (2017). Liquid water infiltration into a layered snowpack: Evaluation of a 3-D water transport model with laboratory experiments. *Hydrology and Earth System Sciences*, *21*(11), 5503–5515. https://doi.org/10.5194/hess-21-5503-2017

Hirashima, H., Yamaguchi, S., & Katsushima, T. (2014). A multi-dimensional water transport model to reproduce preferential flow in the snowpack. *Cold Regions Science and Technology*, *108*, 80–90. https://doi.org/10.1016/j.coldregions.2014.09.004

Hock, R. (2003). Temperature index melt modelling in mountain areas. *Journal of Hydrology*, *282*(1–4), 104–115. https://doi.org/10.1016/S0022-1694(03)00257-9

Hock, R. (2005). Glacier melt: A review of processes and their modelling. *Progress in Physical Geography*, *29*(3), 362–391. https://doi.org/10.1191/0309133305pp453ra

Huber, C. J., Eichler, A., Brütsch, S., Jenk, T. M., Gabrieli, J., Barbante, C., & Schwikowski, M. (2020). Melting influenced signal preservation at Grand Combin Glacier. In M. Schwikowski & M. Ammann (Eds.), *Laboratory of Environmental Chemistry Annual Report 2020* (pp. 25–25). Paul Scherrer Institut.

Humphrey, N. F., Harper, J. T., & Meierbachtol, T. W. (2021). Physical limits to meltwater penetration in firn. *Journal of Glaciology*, *67*(265), 952–960. https://doi.org/10.1017/jog.2021.44

Humphrey, N. F., Harper, J. T., & Pfeffer, W. T. (2012). Thermal tracking of meltwater retention in Greenland's accumulation area. *Journal of Geophysical Research: Earth Surface*, *117*(1). https://doi.org/10.1029/2011JF002083

Iizuka, Y., Igarashi, M., Kamiyama, K., Motoyama, H., & Watanabe, O. (2002). Ratios of Mg2+/Na+ in snowpack and an ice core at Austfonna ice cap, Svalbard, as an indicator of seasonal melting. *Journal of Glaciology*, *48*(162), 452–460. https://doi.org/10.3189/172756502781831304

IPCC. (2019). *IPCC Special Report on the Ocean and Cryosphere in a Changing Climate* (H. Pörtner, D. Roberts, V. Masson-Delmotte, P. Zhai, M. Tignor, E. Poloczanska, K. Mintenbeck, A. Alegría, M. Nicolai, A. Okem, J. Petzold, B. Rama, & N. Weyer, Eds.). Cambridge University Press. https://doi.org/10.1017/9781009157964

IPCC. (2021). Climate Change 2021: The Physical Science Basis. Contribution of Working Group I to the Sixth Assessment Report of the Intergovernmental Panel on Climate Change. In V. Masson-Delmotte, P. Zhai, A. Pirani, S. L. Connors, C. Péan, S. Berger, N. Caud, Y. Chen, L. Goldfarb, M. I. Gomis, M. Huang, K. Leitzell, E. Lonnoy, J. B. R. Matthews, T. K. Maycock, T. Waterfield, O. Yelekçi, R. Yu, & B. Zhou (Eds.), *Climate Change 2021 – The Physical Science Basis*. Cambridge University Press. https://doi.org/10.1017/9781009157896

Jennings, K. S., Kittel, T. G. F., & Molotch, N. P. (2018). Observations and simulations of the seasonal evolution of snowpack cold content and its relation to snowmelt and the snowpack energy budget. *Cryosphere*, *12*(5), 1595–1614. https://doi.org/10.5194/tc-12-1595-2018

Johannessen, M., Dale, T., Gjessing, E. T., Henriksen, A., & Wright, R. F. (1977). Acid precipitation in Norway: the regional distribution of contaminants in snow and the chemical concentration processes during snowmelt. *IAHS Publication*, *118*, 116–120.

Johannessen, M., & Henriksen, A. (1978). Chemistry of Snow Meltwater: Changes in Concentration During Melting. *Water Resources Research*, *14*(4), 615–619. https://doi.org/10.1029/WR014i004p00615

Kaczmarska, M., Isaksson, E., Karlöf, L., Brandt, O., Winther, J. G., Van De Wal, R. S. W., Van Den Broeke, M., & Johnsen, S. J. (2006). Ice core melt features in relation to Antarctic coastal climate. *Antarctic Science*, *18*(2), 271–278. https://doi.org/10.1017/S0954102006000319

Kameda, T., Narita, H., Shoji, H., Nishio, F., Fujii, Y., & Watanabe, O. (1995). Melt features in ice cores from Site J, southern Greenland: some implications for summer climate since AD 1550. *Annals of Glaciology*, *21*, 51–58. https://doi.org/10.3189/S0260305500015597

Kang, S., Huang, J., & Xu, Y. (2008). Changes in ionic concentrations and δ18O in the snowpack of Zhadang glacier, Nyainqentanglha mountain, southern Tibetan Plateau. *Annals of Glaciology*, *49*, 127–134. https://doi.org/10.3189/172756408787814708

Kaspari, S., McKenzie Skiles, S., Delaney, I., Dixon, D., & Painter, T. H. (2015). Accelerated glacier melt on Snow Dome, Mount Olympus, Washington, USA, due to deposition of black carbon and mineral dust from wildfire. *Journal of Geophysical Research: Atmospheres*, *120*(7), 2793–2807. https://doi.org/https://doi.org/10.1002/2014JD022676

Kawakami, K., Iizuka, Y., Matoba, S., Aoki, T., & Ando, T. (2022). Inclusions in ice layers formed by melting and refreezing processes in a Greenland ice core. *Journal of Glaciology*, 1–13. https://doi.org/10.1017/jog.2022.101

Keegan, K. M., Albert, M. R., McConnell, J. R., & Baker, I. (2014). Climate change and forest fires synergistically drive widespread melt events of the Greenland Ice Sheet. *Proceedings of the National Academy of Sciences of the United States of America*, *111*(22), 7964–7967. https://doi.org/10.1073/pnas.1405397111

1075   Keegan, K. M., Albert, M. R., Mcconnell, J. R., & Baker, I. (2019). Climate Effects on Firn Permeability Are Preserved Within a Firn Column. *Journal of Geophysical Research: Earth Surface*, *124*(3), 830–837. https://doi.org/10.1029/2018JF004798

Kinnard, C., Koerner, R. M., Zdanowicz, C. M., Fisher, D. A., Zheng, J., Sharp, M. J., Nicholson, L., & Lauriol, B. (2008). Stratigraphic analysis of an ice core from the Prince of Wales Icefield, Ellesmere Island, Arctic Canada, using digital

1080   image analysis: High-resolution density, past summer warmth reconstruction, and melt effect on ice core solid conductivity. *Journal of Geophysical Research Atmospheres*, *113*(24), 1–14. https://doi.org/10.1029/2008JD011083

Koenig, L. S., Miège, C., Forster, R. R., & Brucker, L. (2014). Initial in situ measurements of perennial meltwater storage in the Greenland firn aquifer. *Geophysical Research Letters*, *41*(1), 81–85. https://doi.org/10.1002/2013GL058083

Koerner, R. M. (1970). Some Observations on Superimposition of Ice on the Devon Island Ice Cap, N.W.T. Canada.

1085   *Geografiska Annaler: Series A, Physical Geography*, *52*(1), 57–67. https://doi.org/10.1080/04353676.1970.11879808

Koerner, R. M. (1977a). Devon Island Ice Cap: Core Stratigraphy and Paleoclimate. *Science*, *196*(4285), 15–18. https://doi.org/10.1126/science.196.4285.15

Koerner, R. M. (1977b). Distribution of microparticles in a 299-m core through the Devon Island ice cap. Northwest Territories, Canada. *International Association of Hydrological Sciences Publication*, *118*, 371–376.

1090   Koerner, R. M. (1989). Ice Core Evidence for Extensive Melting of the Greenland Ice Sheet in the Last Interglacial. *Science*, *244*(4907), 964–968. https://doi.org/10.1126/science.244.4907.964

Koerner, R. M. (1997). Some comments on climatic reconstructions from ice cores drilled in areas of high melt. *Journal of Glaciology*, *43*(143), 90–97. https://doi.org/10.3189/S0022143000002847

Koerner, R. M., & Fisher, D. A. (1990). A record of Holocene summer climate from a Canadian high-Arctic ice core. *Nature*,

1095   *343*(6259), 630–631. https://doi.org/10.1038/343630a0

Koerner, R. M., Paterson, W. S. B., & Krouse, H. R. (1973). δ18O Profile in Ice formed between the Equilibrium and Firn Lines. *Nature Physical Science*, *245*(148), 137–140.

Koh, G., & Jordan, R. (1995). Sub-surface melting in a seasonal snow cover. *Journal of Glaciology*, *41*(139), 474–482. https://doi.org/10.1017/S002214300003481X

1100   Krenke, A. N., & Khodakov, V. G. (1966). O svyazi poverkhnostnogo tayaniya lednikov s temperaturoyi vozdukha (About the relation between surface ablation of the glaciers and the air temperature). *Materialy Glyaciologicheskikh Issledovaniyi, Khronika, Ohsuzhdeniya*, *12*, 153–164.

Kuhn, M. (2001). The nutrient cycle through snow and ice, a review. *Aquatic Sciences*, *63*(2), 150–167. https://doi.org/10.1007/PL00001348

1105   Kuipers-Munneke, P., Ligtenberg, S. R. M., Van Den Broeke, M. R., Van Angelen, J. H., & Forster, R. R. (2014). Explaining the presence of perennial liquid water bodies in the firn of the Greenland Ice Sheet. *Geophysical Research Letters*, *41*(2), 476–483. https://doi.org/10.1002/2013GL058389

Langway, C. C., & Shoji, H. (1990). Past Temperature Record From The Analysis of Melt Features In The Dye 3, Greenland, Ice Core. *Annals of Glaciology*, *14*, 343–344. https://doi.org/10.3189/S0260305500009095

1110 Laska, M., Luks, B., & Budzik, T. (2016). Influence of snowpack internal structure on snow metamorphism and melting intensity on Hansbreen, Svalbard. *Polish Polar Research*, *37*(2), 193–218. https://doi.org/10.1515/popore-2016-0012

Lee, J., Hur, S. Do, Lim, H. S., & Jung, H. (2020). Isotopic characteristics of snow and its meltwater over the Barton Peninsula, Antarctica. *Cold Regions Science and Technology*, *173*, 1–6. https://doi.org/10.1016/j.coldregions.2020.102997

Lenaerts, J. T. M., Lhermitte, S., Drews, R., Ligtenberg, S. R. M., Berger, S., Helm, V., Smeets, C. J. P. P., Broeke, M. R. V.
1115 Den, Van De Berg, W. J., Van Meijgaard, E., Eijkelboom, M., Eisen, O., & Pattyn, F. (2017). Meltwater produced by wind-albedo interaction stored in an East Antarctic ice shelf. *Nature Climate Change*, *7*(1), 58–62. https://doi.org/10.1038/nclimate3180

Leroux, N. R., & Pomeroy, J. W. (2017). Modelling capillary hysteresis effects on preferential flow through melting and cold layered snowpacks. *Advances in Water Resources*, *107*, 250–264. https://doi.org/10.1016/j.advwatres.2017.06.024

1120 Li, Z., Edwards, R., Mosley-Thompson, E., Wang, F., Dong, Z., You, X., Li, H., Li, C., & Zhu, Y. (2006). Seasonal variability of ionic concentrations in surface snow and elution processes in snow-firn packs at the PGPI site on Ürümqi glacier No. 1, eastern Tien Shan, China. *Annals of Glaciology*, *43*, 250–256. https://doi.org/10.3189/172756406781812069

Ligtenberg, S. R. M., Helsen, M. M., & Van Den Broeke, M. R. (2011). An improved semi-empirical model for the densification of Antarctic firn. *Cryosphere*, *5*(4), 809–819. https://doi.org/10.5194/tc-5-809-2011

1125 Lliboutry, L. (1996). Temperate ice permeability, stability of water veins and percolation of internal meltwater. *Journal of Glaciology*, *42*(141), 201–211. https://doi.org/10.3189/S0022143000004068

Macdonell, S., Fernandoy, F., Villar, P., & Hammann, A. (2021). Stratigraphic Analysis of Firn Cores from an Antarctic Ice Shelf Firn Aquifer. *Water (Switzerland)*, *13*(5), 731. https://doi.org/10.3390/w13050731

Machguth, H., Macferrin, M., Van As, D., Box, J. E., Charalampidis, C., Colgan, W., Fausto, R. S., Meijer, H. A. J., Mosley-
1130 Thompson, E., & Van De Wal, R. S. W. (2016). Greenland meltwater storage in firn limited by near-surface ice formation. *Nature Climate Change*, *6*(4), 390–393. https://doi.org/10.1038/nclimate2899

Marsh, P., & Woo, M.-K. (1984). Wetting Front Advance and Freezing of Meltwater Within a Snow Cover 1. Observations in the Canadian Arctic. *Water Resources Research*, *20*(12), 1853–1864. https://doi.org/10.1029/WR020i012p01853

Martinerie, P., Raynaud, D., Etheridge, D. M., Barnola, J.-M., & Mazaudier, D. (1992). Physical and climatic parameters
1135 which influence the air content in polar ice. *Earth and Planetary Science Letters*, *112*, 1–13. https://doi.org/10.1016/0012-821X(92)90002-D

Matsuoka, K., & Naruse, R. (1999). Mass Balance Features Derived from a Firn Core at Hielo Patagónico Norte, South America. *Arctic, Antarctic, and Alpine Research*, *31*(4), 333–340. https://doi.org/10.1080/15230430.1999.12003318

Mattea, E., MacHguth, H., Kronenberg, M., Van Pelt, W., Bassi, M., & Hoelzle, M. (2021). Firn changes at Colle Gnifetti
1140 revealed with a high-resolution process-based physical model approach. *Cryosphere*, *15*(7), 3181–3205. https://doi.org/10.5194/tc-15-3181-2021

Mattson, L. E., Gardner, J. S., & Young, G. J. (1993). Ablation on Debris Covered Glaciers: an Example from the Rakhiot Glacier, Punjab, Himalaya. *IAHS Publication*, *218*, 289–296.

McDowell, I. E., Keegan, K. M., Wever, N., Osterberg, E. C., Hawley, R. L., & Marshall, H. (2023). Firn core evidence of two-way feedback mechanisms between meltwater percolation and firn microstructure from the western percolation zone of the Greenland Ice Sheet. *Journal of Geophysical Research: Earth Surface*, *128*(e2022JF006752), 1–18. https://doi.org/10.1029/2022jf006752

McGurk, B. J., & Kattelmann, R. C. (1988). Evidence of liquid water flow through snow from thick-section photography. *International Snow Science Workshop, Canadian Avalanche Association*, 137–139.

McLeod, J. T., & Mote, T. L. (2016). Linking interannual variability in extreme Greenland blocking episodes to the recent increase in summer melting across the Greenland ice sheet. *International Journal of Climatology*, *36*(3), 1484–1499. https://doi.org/10.1002/joc.4440

Meyer, C. R., & Hewitt, I. J. (2017). A continuum model for meltwater flow through compacting snow. *Cryosphere*, *11*(6), 2799–2813. https://doi.org/10.5194/tc-11-2799-2017

Meyer, T., & Wania, F. (2011). Modeling the elution of organic chemicals from a melting homogeneous snow pack. *Water Research*, *45*(12), 3627–3637. https://doi.org/10.1016/j.watres.2011.04.011

Miller, O., Solomon, D. K., Miège, C., Koenig, L., Forster, R., Schmerr, N., Ligtenberg, S. R. M., Legchenko, A., Voss, C. I., Montgomery, L., & McConnell, J. R. (2020). Hydrology of a Perennial Firn Aquifer in Southeast Greenland: An Overview Driven by Field Data. *Water Resources Research*, *56*(8). https://doi.org/10.1029/2019WR026348

Mitchell, L. E., Buizert, C., Brook, E. J., Breton, D. J., Fegyveresi, J., Baggenstos, D., Orsi, A., Severinghaus, J., Alley, R. B., Albert, M., Rhodes, R. H., McConnell, J. R., Sigl, M., Maselli, O., Gregory, S., & Ahn, J. (2015). Observing and modeling the influence of layering on bubble trapping in polar firn. *Journal of Geophysical Research*, *120*(6), 2558–2574. https://doi.org/10.1002/2014JD022766

Moore, J. C., & Grinsted, A. (2009). Ion fractionation and percolation in ice cores with seasonal melting. In T. Hondoh (Ed.), *Physics of Ice Core Records II: Papers collected after the 2nd International Workshop on Physics of Ice Core Records* (68th ed.).

Moore, J. C., Grinsted, A., Kekonen, T., & Pohjola, V. (2005). Separation of melting and environmental signals in an ice core with seasonal melt. *Geophysical Research Letters*, *32*(10), 1–4. https://doi.org/10.1029/2005GL023039

Moran, T., & Marshall, S. (2009). The effects of meltwater percolation on the seasonal isotopic signals in an Arctic snowpack. *Journal of Glaciology*, *55*(194), 1012–1024. https://doi.org/10.3189/002214309790794896

Moser, D. E., Jackson, S., Kjær, H. A., Markle, B. R., Ngoumtsa, E., Pedro, J. B., Segato, D., Spolaor, A., Tetzner, D., Vallelonga, P., & Thomas, E. R. (2021). An Age Scale for the First Shallow (Sub-)Antarctic Ice Core from Young Island, Northwest Ross Sea. *Geosciences*, *11*(368), 1–18. https://doi.org/10.3390/geosciences11090368

Müller-Tautges, C., Eichler, A., Schwikowski, M., Pezzatti, G. B., Conedera, M., & Hoffmann, T. (2016). Historic records of organic compounds from a high Alpine glacier: Influences of biomass burning, anthropogenic emissions, and dust transport. *Atmospheric Chemistry and Physics*, *16*(2), 1029–1043. https://doi.org/10.5194/acp-16-1029-2016

Munneke, P. K., Ligtenberg, S. R. M., Van Den Broeke, M. R., & Vaughan, D. G. (2014). Firn air depletion as a precursor of Antarctic ice-shelf collapse. *Journal of Glaciology*, *60*(220), 205–214. https://doi.org/10.3189/2014JoG13J183

NEEM community members. (2013). Eemian interglacial reconstructed from a Greenland folded ice core. *Nature*, *493*(7433), 489–494. https://doi.org/10.1038/nature11789

Neff, P. D. (2014). A review of the brittle ice zone in polar ice cores. In *Annals of Glaciology* (Vol. 55, Issue 68, pp. 72–82). International Glaciology Society. https://doi.org/10.3189/2014AoG68A023

Neff, P. D., Steig, E. J., Clark, D. H., McConnell, J. R., Pettit, E. C., & Menounos, B. (2012). Ice-core net snow accumulation and seasonal snow chemistry at a temperate-glacier site: Mount Waddington, southwest British Columbia, Canada. *Journal of Glaciology*, *58*(212), 1165–1175. https://doi.org/10.3189/2012JoG12J078

Neff, W. (2018). Atmospheric rivers melt Greenland. *Nature Climate Change*, *8*(October), 857–858.

Neftel, A., Oeschger, H., Schwander, J., & Stauffer, B. (1983). Carbon Dioxide Concentration in Bubbles of Natural Cold Ice. *Journal of Physical Chemistry*, *87*(21), 4116–4120. https://doi.org/10.1021/j100244a025

Nghiem, S. V., Hall, D. K., Mote, T. L., Tedesco, M., Albert, M. R., Keegan, K., Shuman, C. A., DiGirolamo, N. E., & Neumann, G. (2012). The extreme melt across the Greenland ice sheet in 2012. *Geophysical Research Letters*, *39*(20), 1–6. https://doi.org/10.1029/2012GL053611

Nicolas, J. P., Vogelmann, A. M., Scott, R. C., Wilson, A. B., Cadeddu, M. P., Bromwich, D. H., Verlinde, J., Lubin, D., Russell, L. M., Jenkinson, C., Powers, H. H., Ryczek, M., Stone, G., & Wille, J. D. (2017). January 2016 extensive summer melt in West Antarctica favoured by strong El Niño. *Nature Communications*, *8*(15799). https://doi.org/10.1038/ncomms15799

Niwano, M., Box, J. E., Wehrlé, A., Vandecrux, B., Colgan, W. T., & Cappelen, J. (2021). Rainfall on the Greenland Ice Sheet: Present-Day Climatology From a High-Resolution Non-Hydrostatic Polar Regional Climate Model. *Geophysical Research Letters*, *48*(15). https://doi.org/10.1029/2021GL092942

Nye, J. F. (1998). Diffusion of isotopes in the annual layers of ice sheets. *Journal of Glaciology*, *44*(148), 467–468. https://doi.org/10.3189/S0022143000001982

Okamoto, S., Fujita, K., Narita, H., Uetake, J., Takeuchi, N., Miyake, T., Nakazawa, F., Aizen, V. B., Nikitin, S. A., & Nakawo, M. (2011). Reevaluation of the reconstruction of summer temperatures from melt features in Belukha ice cores, Siberian Altai. *Journal of Geophysical Research: Atmospheres*, *116*(D2), 1–11. https://doi.org/https://doi.org/10.1029/2010JD013977

Olson, M., & Rupper, S. (2019). Impacts of topographic shading on direct solar radiation for valley glaciers in complex topography. *Cryosphere*, *13*(1), 29–40. https://doi.org/10.5194/tc-13-29-2019

Orsi, A. J., Kawamura, K., Fegyveresi, J. M., Headly, M. A., Alley, R. B., & Severinghaus, J. P. (2015). Differentiating bubble-free layers from melt layers in ice cores using noble gases. *Journal of Glaciology*, *61*(227), 585–594. https://doi.org/10.3189/2015jog14j237

1210 Osmont, D., Brugger, S., Gilgen, A., Weber, H., Sigl, M., Modini, R., Schwörer, C., Tinner, W., Wunderle, S., & Schwikowski, M. (2020). Tracing devastating fires in Portugal to a snow archive in the Swiss Alps: a case study. *The Cryosphere Discussions*, 1–27. https://doi.org/10.5194/tc-2020-58

Osmont, D., Wendl, I. A., Schmidely, L., Sigl, M., Vega, C. P., Isaksson, E., & Schwikowski, M. (2018). An 800-year high-resolution black carbon ice core record from Lomonosovfonna, Svalbard. *Atmospheric Chemistry and Physics*, *18*(17),
1215 12777–12795. https://doi.org/10.5194/acp-18-12777-2018

Pang, H., He, Y., Hou, S., & Zhang, N. (2012). Changes in ionic and oxygen isotopic composition of the snow-firn pack at Baishui Glacier No. 1, southeastern Tibetan Plateau. *Environmental Earth Sciences*, *67*(8), 2345–2358. https://doi.org/10.1007/s12665-012-1681-4

Parlange, J.-Y. (1974). Water movement in soils. *Geophysical Surveys*, *1*, 357–387. https://doi.org/10.1007/BF01449119

1220 Pavlova, P. A., Jenk, T. M., Schmid, P., Bogdal, C., Steinlin, C., & Schwikowski, M. (2015). Polychlorinated Biphenyls in a Temperate Alpine Glacier: 1. Effect of Percolating Meltwater on their Distribution in Glacier Ice. *Environmental Science and Technology*, *49*(24), 14085–14091. https://doi.org/10.1021/acs.est.5b03303

Pfeffer, W. T., & Humphrey, N. F. (1996). Determination of timing and location of water movement and ice-layer formation by temperature measurements in sub-freezing snow. *Journal of Glaciology*, *42*(141), 292–304.
1225 https://doi.org/10.3189/S0022143000004159

Pfeffer, W. T., & Humphrey, N. F. (1998). Formation of ice layers by infiltration and refreezing of meltwater. *Annals of Glaciology*, *26*, 83–91. https://doi.org/10.3189/1998aog26-1-83-91

Pfeffer, W. T., Meier, M. F., & Illangasekare, T. H. (1991). Retention of Greenland runoff by refreezing: implications for projected future sea level change. *Journal of Geophysical Research*, *96*(C12). https://doi.org/10.1029/91jc02502

1230 Pinglot, J. F., Vaikmäe, R. A., Kamiyama, K., Igarashi, M., Fritzsche, D., Wilhelms, F., Koerner, R., Henderson, L., Isaksson, E., Winther, J. G., Van De Wal, R. S. W., Fournier, M., Bouisset, P., & Meijer, H. A. J. (2003). Ice cores from Arctic sub-polar glaciers: Chronology and post-depositional processes deduced from radioactivity measurements. *Journal of Glaciology*, *49*(164), 149–158. https://doi.org/10.3189/172756503781830944

Plach, A., Vinther, B., H. Nisancioglu, K., Vudayagiri, S., & Blunier, T. (2021). Greenland climate simulations show high
1235 Eemian surface melt which could explain reduced total air content in ice cores. *Climate of the Past*, *17*(1), 317–330. https://doi.org/10.5194/cp-17-317-2021

Pohjola, V. A., Moore, J. C., Isaksson, E., Jauhiainen, T., van de Wal, R. S. W., Martma, T., Meijer, H. A. J., & Vaikmäe, R. (2002). Effect of periodic melting on geochemical and isotopic signals in an ice core from Lomonosovfonna, Svalbard. *Journal of Geophysical Research*, *107*(D4), 1–14. https://doi.org/10.1029/2000JD000149

1240   Porter, S. E., Mosley-Thompson, E., Thompson, L. G., & Wilson, A. B. (2021). Reconstructing an Interdecadal Pacific Oscillation Index from a Pacific Basin–Wide Collection of Ice Core Records. *Journal of Climate*, *34*(10), 3839–3852. https://doi.org/10.1175/JCLI-D-20-0455.1

Rempel, A., Waddington, E., Wettlaufer, J., & Worster, M. G. (2001). Possible displacement of the climate signal in ancient ice by premelting and anomalous diffusion. *Nature*, *471*, 568–571. https://doi.org/10.1038/35079043

1245   Reznichenko, N., Davies, T., Shulmeister, J., & McSaveney, M. (2010). Effects of debris on ice-surface melting rates: an experimental study. *Journal of Glaciology*, *56*(197), 384–394. https://doi.org/DOI: 10.3189/002214310792447725

Roberts, J., Moy, A., Plummer, C., Ommen, T. van, Curran, M. A. J., Vance, T. R., Poynter, S., Liu, Y., Pedro, J., Treverrow, A., Tozer, C., Jong, L., Whitehouse, P., Loulergue, L., Chappellaz, J., Morgan, V., Spahni, R., Schilt, A., Meure, C. M., … Stocker, T. (2017). A revised Law Dome age model (LD2017) and implications for last glacial climate. *Climate of*
1250   *the Past Discussions*, *August*, 1–22. https://doi.org/10.5194/cp-2017-96

Rowan, A. V., Nicholson, L. I., Quincey, D. J., Gibson, M. J., Irvine-Fynn, T. D. L., Watson, C. S., Wagnon, P., Rounce, D. R., Thompson, S. S., Porter, P. R., & Glasser, N. F. (2021). Seasonally stable temperature gradients through supraglacial debris in the Everest region of Nepal, Central Himalaya. *Journal of Glaciology*, *67*(261), 170–181. https://doi.org/10.1017/jog.2020.100

1255   Samimi, S., Marshall, S. J., & MacFerrin, M. (2020). Meltwater Penetration Through Temperate Ice Layers in the Percolation Zone at DYE-2, Greenland Ice Sheet. *Geophysical Research Letters*, *47*(15), 1–9. https://doi.org/10.1029/2020GL089211

Sánchez, M. A., Kling, T., Ishiyama, T., Van Zadel, M. J., Bisson, P. J., Mezger, M., Jochum, M. N., Cyran, J. D., Smit, W. J., Bakker, H. J., Shultz, M. J., Morita, A., Donadio, D., Nagata, Y., Bonn, M., & Backus, E. H. G. (2017). Experimental
1260   and theoretical evidence for bilayer-by-bilayer surface melting of crystalline ice. *Proceedings of the National Academy of Sciences*, *114*(2), 227–232. https://doi.org/10.1073/pnas.1612893114

Schilt, A., Baumgartner, M., Blunier, T., Schwander, J., Spahni, R., Fischer, H., & Stocker, T. F. (2010). Glacial-interglacial and millennial-scale variations in the atmospheric nitrous oxide concentration during the last 800,000 years. *Quaternary Science Reviews*, *29*(1–2), 182–192. https://doi.org/10.1016/j.quascirev.2009.03.011

1265   Schilt, A., Baumgartner, M., Schwander, J., Buiron, D., Capron, E., Chappellaz, J., Loulergue, L., Schüpbach, S., Spahni, R., Fischer, H., & Stocker, T. F. (2010). Atmospheric nitrous oxide during the last 140,000years. *Earth and Planetary Science Letters*, *300*(1–2), 33–43. https://doi.org/10.1016/j.epsl.2010.09.027

Schöndorf, T., & Herrmann, R. (1987). Transport and Chemodynamics of Organic Micropollutants and Ions during Snowmelt. *Nordic Hydrology*, *18*(4–5), 259–278. https://doi.org/10.2166/nh.1987.0019

1270   Schwander, J., & Stauffer, B. (1984). Age difference between polar ice and the air trapped in its bubbles. *Nature*, *311*, 276–279. https://doi.org/10.1038/311045a0

Schwikowski, M., Schläppi, M., Santibañez, P., Rivera, A., & Casassa, G. (2013). Net accumulation rates derived from ice core stable isotope records of Pío XI glacier, Southern Patagonia Icefield. *Cryosphere*, *7*(5), 1635–1644. https://doi.org/10.5194/tc-7-1635-2013

Scott, R. C., Nicolas, J. P., Bromwich, D. H., Norris, J. R., & Lubin, D. (2019). Meteorological drivers and large-scale climate forcing of West Antarctic surface melt. *Journal of Climate*, *32*(3), 665–684. https://doi.org/10.1175/JCLI-D-18-0233.1

Shiraiwa, T., Kohshima, S., Uemura, R., Yoshida, N., Matoba, S., Uetake, J., & Godoi, M. A. (2002). High net accumulation rates at Campo de Hielo Patagónico Sur, South America, revealed by analysis of a 45.97 m long ice core. *Annals of Glaciology*, *35*, 84–90. https://doi.org/10.3189/172756402781816942

Simmleit, N., Herrmann, R., & Thomas, S. W. (1986). Chemical behaviour of hydrophobic micro-pollutants during the melting of snow. *IAHS Publication Series*, *155*, 335–346.

Sinclair, K. E., & MacDonell, S. (2016). Seasonal evolution of penitente glaciochemistry at Tapado Glacier, Northern Chile. *Hydrological Processes*, *30*(2), 176–186. https://doi.org/10.1002/hyp.10531

Slater, B., & Michaelides, A. (2019). Surface premelting of water ice. In *Nature Reviews Chemistry* (Vol. 3, Issue 3, pp. 172–188). Nature Publishing Group. https://doi.org/10.1038/s41570-019-0080-8

Sommer, C. G., Wever, N., Fierz, C., & Lehning, M. (2018). Wind-packing of snow in Antarctica. *The Cryosphere Discussions*, 1–11. https://doi.org/10.5194/tc-2018-36

Sommers, A. N., Rajaram, H., Weber, E. P., Macferrin, M. J., Colgan, W., & Stevens, C. M. (2017). Inferring firn permeability from pneumatic testing: A case study on the Greenland ice sheet. *Frontiers in Earth Science*, *5*. https://doi.org/10.3389/feart.2017.00020

Souchez, R. A., & Jouzel, J. (1984). On the Isotopic Composition in δD and δ18O of Water and Ice During Freezing. *Journal of Glaciology*, *30*(106), 369–372. https://doi.org/10.3189/S0022143000006249

Spolaor, A., Scoto, F., Larose, C., Barbaro, E., Burgay, F., Cappelletti, D., Dallo, F., de Blasi, F., Divine, D., Gabrieli, J., Isaksson, E., Kohler, J., Martma, T., Schmidt, L. S., Schuler, T. V, Stenni, B., Turetta, C., Luks, B., Casado, M., & Gallet, J.-C. (2023). Climate change is rapidly deteriorating the climatic signal in Svalbard glaciers. *The Cryosphere Discussions*, 1–24. https://doi.org/10.5194/tc-2023-96

Spolaor, A., Varin, C., Pedeli, X., Christille, J. M., Kirchgeorg, T., Giardi, F., Cappelletti, D., Turetta, C., Cairns, W. R. L., Gambaro, A., Bernagozzi, A., Gallet, J. C., Björkman, M. P., & Barbaro, E. (2021). Source, timing and dynamics of ionic species mobility in the Svalbard annual snowpack. *Science of the Total Environment*, *751*. https://doi.org/10.1016/j.scitotenv.2020.141640

Stauffer, B., Neftel, A., Oeschger, H., & Schwander, J. (1985). CO2 Concentration in Air Extracted from Greenland Ice Samples. *Geophysical Monograph Series: Greenland Ice Core: Geophysics, Geochemistry, and the Environment*, *33*. https://doi.org/10.1029/GM033p0085

Svensson, A., Nielsen, S. W., Kipfstuhl, S., Johnsen, S. J., Steffensen, J. P., Bigler, M., Ruth, U., & Röthlisberger, R. (2005). Visual stratigraphy of the North Greenland Ice Core Project (NorthGRIP) ice core during the last glacial period. *Journal of Geophysical Research D: Atmospheres*, *110*(2), 1–11. https://doi.org/10.1029/2004JD005134

Takeuchi, N., Sera, S., Fujita, K., Aizen, V. B., & Kubota, J. (2019). Annual layer counting using pollen grains of the Grigoriev ice core from the Tien Shan Mountains, central Asia. *Arctic, Antarctic, and Alpine Research*, *51*(1), 299–312. https://doi.org/10.1080/15230430.2019.1638202

Taranczewski, T., Freitag, J., Eisen, O., Vinther, B., Wahl, S., & Kipfstuhl, S. (2019). 10,000 years of melt history of the 2015 Renland ice core, East Greenland. *The Cryosphere Discussions*. https://doi.org/10.5194/tc-2018-280

Tarussov, A. (1992). The Arctic from Svalbard to Severnaya Zemblya: Climatic reconstruction from ice cores. *Climate since AD 1500*, 505–516.

Taylor, S., Feng, X., Kirchner, J. W., Osterhuber, R., Klaue, B., & Renshaw, C. E. (2001). Isotopic evolution of a seasonal snowpack and its melt. *Water Resources Research*, *37*(3), 759–769. https://doi.org/10.1029/2000WR900341

Tedesco, M., & Fettweis, X. (2020). Unprecedented atmospheric conditions (1948-2019) drive the 2019 exceptional melting season over the Greenland ice sheet. *Cryosphere*, *14*(4), 1209–1223. https://doi.org/10.5194/tc-14-1209-2020

Thackeray, C. W., & Fletcher, C. G. (2016). Snow albedo feedback: Current knowledge, importance, outstanding issues and future directions. *Progress in Physical Geography*, *40*(3), 392–408. https://doi.org/10.1177/0309133315620999

Thomas, E. R., Allen, C. S., Etourneau, J., King, A. C. F., Severi, M., Winton, V. H. L., Mueller, J., Crosta, X., & Peck, V. L. (2019). Antarctic sea ice proxies from marine and ice core archives suitable for reconstructing sea ice over the past 2000 years. In *Geosciences* (Vol. 9, Issue 12, pp. 506–539). MDPI AG. https://doi.org/10.3390/geosciences9120506

Thomas, E. R., Gacitúa, G., Pedro, J. B., King, A. C. F., Markle, B., Potocki, M., & Moser, D. E. (2021). Physical properties of shallow ice cores from Antarctic and sub-Antarctic islands. *The Cryosphere*, *15*(2), 1173–1186. https://doi.org/10.5194/tc-15-1173-2021

Thompson, L. G., Davis, M. E., Mosley-Thompson, E., Porter, S. E., Corrales, G. V., Shuman, C. A., & Tucker, C. J. (2021). The impacts of warming on rapidly retreating high-altitude, low-latitude glaciers and ice core-derived climate records. *Global and Planetary Change*, *203*. https://doi.org/10.1016/j.gloplacha.2021.103538

Thompson, L. G., Mosley-Thompson, E., Davis, M., Lin, P. N., Yao, T., Dyurgerov, M., & Dai, J. (1993). "Recent warming": ice core evidence from tropical ice cores with emphasis on Central Asia. *Global and Planetary Change*, *7*(1–3), 145–156. https://doi.org/10.1016/0921-8181(93)90046-Q

Trachsel, J. C., Avak, S. E., Edebeli, J., Schneebeli, M., Bartels-Rausch, T., Bruetsch, S., & Eichler, A. (2019). Microscale Rearrangement of Ammonium Induced by Snow Metamorphism. *Frontiers in Earth Science*, *7*. https://doi.org/10.3389/feart.2019.00194

Tranter, M., Brimblecombe, P., Davies, T. D., Vincent, C. E., Abrahams, P. W., & Blackwood, I. (1986). The composition of snowfall, snowpack and meltwater in the Scottish highlands-evidence for preferential elution. *Atmospheric Environment*, *20*(3), 517–525. https://doi.org/10.1016/0004-6981(86)90092-2

Tranter, M., Tsiouris, S., Davies, T. D., & Jones, H. G. (1992). A laboratory investigation of the leaching of solute from snowpack by rainfall. *Hydrological Processes*, 6, 169–178. https://doi.org/10.1002/hyp.3360060205

Trudinger, C. M., Enting, I. G., Etheridge, D. M., Francey, R. J., Levchenko, V. A., Steele, L. P., Raynaud, D., & Arnaud, L. (1997). Modeling air movement and bubble trapping in firn. *Journal of Geophysical Research Atmospheres*, *102*(D6), 6747–6763. https://doi.org/10.1029/96JD03382

Trusel, L. D., Frey, K. E., Das, S. B., Karnauskas, K. B., Kuipers Munneke, P., Van Meijgaard, E., & Van Den Broeke, M. R. (2015). Divergent trajectories of Antarctic surface melt under two twenty-first-century climate scenarios. *Nature Geoscience*, *8*(12), 927–932. https://doi.org/10.1038/ngeo2563

Tschumi, J., & Stauffer, B. (2000). Reconstructing past atmospheric CO2 concentration based on ice-core analyses: Open questions due to in situ production of CO2 in the ice. *Journal of Glaciology*, *46*(152), 45–53. https://doi.org/10.3189/172756500781833359

Tsiouris, S., Vincent, C. E., Davies, T. D., & Brimbleco, P. (1985). The Elution of Ions Through Field and Laboratory Snowpacks. *Annals of Glaciology*, 7, 196–201. https://doi.org/10.3189/S0260305500006169

Van Den Broeke, M. (2005). Strong surface melting preceded collapse of Antarctic Peninsula ice shelf. *Geophysical Research Letters*. https://doi.org/10.1029/2005GL023247

Van Der Wel, L. G., Streurman, H. J., Isaksson, E., Helsen, M. M., Van De Wal, R. S. W., Martma, T., Pohjola, V. A., Moore, J. C., & Meijer, H. A. J. (2011). Using high-resolution tritium profiles to quantify the effects of melt on two Spitsbergen ice cores. *Journal of Glaciology*, *57*(206), 1087–1097.

Van Wessem, J. M., Ligtenberg, S. R. M., Reijmer, C. H., Van De Berg, W. J., Van Den Broeke, M. R., Barrand, N. E., Thomas, E. R., Turner, J., Wuite, J., Scambos, T. A., & Van Meijgaard, E. (2016). The modelled surface mass balance of the Antarctic Peninsula at 5.5 km horizontal resolution. *Cryosphere*, *10*(1), 271–285. https://doi.org/10.5194/tc-10-271-2016

Vandecrux, B., MacFerrin, M., MacHguth, H., Colgan, W. T., Van As, D., Heilig, A., Max Stevens, C., Charalampidis, C., Fausto, R. S., Morris, E. M., Mosley-Thompson, E., Koenig, L., Montgomery, L. N., Miège, C., Simonsen, S. B., Ingeman-Nielsen, T., & Box, J. E. (2019). Firn data compilation reveals widespread decrease of firn air content in western Greenland. *Cryosphere*, *13*(3), 845–859. https://doi.org/10.5194/tc-13-845-2019

Vandecrux, B., Mottram, R., L. Langen, P., S. Fausto, R., Olesen, M., Max Stevens, C., Verjans, V., Leeson, A., Ligtenberg, S., Kuipers Munneke, P., Marchenko, S., Van Pelt, W., R. Meyer, C., B. Simonsen, S., Heilig, A., Samimi, S., Marshall, S., Machguth, H., MacFerrin, M., … E. Box, J. (2020). The firn meltwater Retention Model Intercomparison Project (RetMIP): Evaluation of nine firn models at four weather station sites on the Greenland ice sheet. *Cryosphere*, *14*(11), 3785–3810. https://doi.org/10.5194/tc-14-3785-2020

Vega, C. P., Pohjola, V. A., Beaudon, E., Claremar, B., Van Pelt, W. J. J., Pettersson, R., Isaksson, E., Martma, T., Schwikowski, M., & Bøggild, C. E. (2016). A synthetic ice core approach to estimate ion relocation in an ice field site

experiencing periodical melt: A case study on Lomonosovfonna, Svalbard. *Cryosphere*, *10*(3), 961–976. https://doi.org/10.5194/tc-10-961-2016

Veres, D., Bazin, L., Landais, A., Toyé Mahamadou Kele, H., Lemieux-Dudon, B., Parrenin, F., Martinerie, P., Blayo, E., Blunier, T., Capron, E., Chappellaz, J., Rasmussen, S. O., Severi, M., Svensson, A., Vinther, B., & Wolff, E. W. (2013). The Antarctic ice core chronology (AICC2012): An optimized multi-parameter and multi-site dating approach for the last 120 thousand years. *Climate of the Past*. https://doi.org/10.5194/cp-9-1733-2013

Virkkunen, K., Moore, J. C., Isaksson, E., Pohjola, V., Pera¨ma¨ki, P., Pera¨ma, P., Pera¨ma¨ki, P., Grinsted, A., & Kekonen, T. (2007). Warm summers and ion concentrations in snow: Comparison of present day with Medieval Warm Epoch from snow pits and an ice core from Lomonosovfonna, Svalbard. *Journal of Glaciology*, *53*(183), 623–634. https://doi.org/10.3189/002214307784409388

Vudayagiri, S., Blunier, T., Vinther, B. M., Freitag, J., & Taranczewski, T. (2018). Inferences from the total air content measurements of RECAP ice core. *20th EGU General Assembly, EGU2018, Proceedings from the Conference Held 4-13 April, 2018 in Vienna, Austria*, 1116.

WAIS Divide Project Members. (2013). Onset of deglacial warming in West Antarctica driven by local orbital forcing. *Nature*, *500*(7463), 440–444. https://doi.org/10.1038/nature12376

Wakahama, G. (1968). The Metamorphism of Wet Snow. *International Association of Hydrological Sciences Publication*, *79*, 370–379.

Wakahama, G. (1975). The role of meltwater in densification processes of snow and firn percolation of meltwater into a snow cover. *International Association of Hydrological Sciences Publication*, *114*, 66–72.

Warren, S. G. (2019). Optical properties of ice and snow. In *Philosophical Transactions of the Royal Society A: Mathematical, Physical and Engineering Sciences* (Vol. 377, Issue 2146). Royal Society Publishing. https://doi.org/10.1098/rsta.2018.0161

Watanabe, K., Hirai, T., & Kawada, K. (2015). Ratios of Mg^{2+}/Na^{+} in the snow cover at Murododaira, Mt. Tateyama, Japan: On the possibility of an indicator of chemical leaching. *Bulletin of Glaciological Research*, *33*, 1–5. https://doi.org/10.5331/bgr.33.1

Weiler, K., Fischer, H., Fritzsche, D., Ruth, U., Wilhelms, F., & Miller, H. (2005). Glaciochemical reconnaissance of a new ice core from Severnaya Zemlya, Eurasian Arctic. *Journal of Glaciology*, *51*(172), 64–74. https://doi.org/10.3189/172756505781829629

Weinhart, A. H., Kipfstuhl, S., Hörhold, M., Eisen, O., & Freitag, J. (2021). Spatial Distribution of Crusts in Antarctic and Greenland Snowpacks and Implications for Snow and Firn Studies. *Frontiers in Earth Science*, *9*(March). https://doi.org/10.3389/feart.2021.630070

Weiss, R. F. (1974). Carbon dioxide in water and seawater: the solubility of a non-ideal gas. *Marine Chemistry*, *2*(3), 203–215. https://doi.org/https://doi.org/10.1016/0304-4203(74)90015-2

Westhoff, J., Sinnl, G., Svensson, A., Freitag, J., Kjær, H. A., Vallelonga, P., Vinther, B., Kipfstuhl, S., Dahl-Jensen, D., & Weikusat, I. (2022). Melt in the Greenland EastGRIP ice core reveals Holocene warm events. *Climate of the Past*, *18*(5), 1011–1034. https://doi.org/10.5194/cp-18-1011-2022

Wille, J. D., Favier, V., Dufour, A., Gorodetskaya, I. V., Turner, J., Agosta, C., & Codron, F. (2019). West Antarctic surface melt triggered by atmospheric rivers. *Nature Geoscience*, *12*(11), 911–916. https://doi.org/10.1038/s41561-019-0460-1

Williams, M. W., Erickson, T. A., & Petrzelka, J. L. (2010). Visualizing meltwater flow through snow at the centimetre-to-metre scale using a snow guillotine. *Hydrological Processes*, *24*(15), 2098–2110. https://doi.org/10.1002/hyp.7630

Winski, D., Osterberg, E., Kreutz, K., Wake, C., Ferris, D., Campbell, S., Baum, M., Bailey, A., Birkel, S., Introne, D., & Handley, M. (2018). A 400-Year Ice Core Melt Layer Record of Summertime Warming in the Alaska Range. *Journal of Geophysical Research: Atmospheres*, *123*(7), 3594–3611. https://doi.org/10.1002/2017JD027539

Wong, G. J., Hawley, R. L., Lutz, E. R., & Osterberg, E. C. (2013). Trace-element and physical response to melt percolation in Summit (Greenland) snow. *Annals of Glaciology*, *54*(63), 52–62. https://doi.org/10.3189/2013AoG63A602

Wu, G., Li, P., Zhang, X., & Zhang, C. (2018). Using a geochemical method of dissolved and insoluble fractions to characterize surface snow melting and major element elution. *Journal of Glaciology*, *64*(248), 1003–1013. https://doi.org/10.1038/s41558-020-0827-8

You, X., Li, Z., Edwards, R., & Wang, L. (2015). The transport of chemical components in homogeneous snowpacks on urumqi glacier no. 1, eastern tianshan mountains, central Asia. *Journal of Arid Land*, *7*(5), 612–622. https://doi.org/10.1007/s40333-015-0131-z

Yuanqing, H., Tandong, Y., Guodong, C., & Meixue, Y. (2001). Climatic records in a firn core from an Alpine temperate glacier on Mt. Yulong, southeastern part of the Tibetan Plateau. *Episodes*, *24*(1), 13–18. https://doi.org/10.18814/epiiugs/2001/v24i1/004

Zhang, C., Wu, G., Gao, S., Zhao, Z., Zhang, X., Tian, L., Mu, Y., & Joswiak, D. (2013). Distribution of major elements between the dissolved and insoluble fractions in surface snow at Urumqi Glacier No. 1, Eastern Tien Shan. *Atmospheric Research*, *132–133*, 299–308. https://doi.org/10.1016/j.atmosres.2013.05.009

Zhang, L., Vance, T. R., Fraser, A. D., Jong, L. M., Thompson, S. S., Criscitiello, A. S., & Abram, N. J. (2023). Identifying atmospheric processes favouring the formation of bubble-free layers in the Law Dome ice core, East Antarctica. *Cryosphere*, *17*(12), 5155–5173. https://doi.org/10.5194/tc-17-5155-2023

Zheng, L., Zhou, C., & Wang, K. (2020). Enhanced winter snowmelt in the Antarctic Peninsula: Automatic snowmelt identification from radar scatterometer. *Remote Sensing of Environment*, *246*(September 2019), 1–11. https://doi.org/10.1016/j.rse.2020.111835

Zhongyang, H., Munneke, P. K., Lhermitte, S., Izeboud, M., & van den Broeke, M. (2021). Improving Surface Melt Estimation over Antarctica Using Deep Learning: A Proof-of-Concept over the Larsen Ice Shelf. *The Cryosphere Discuss*, *1*(April), 1–29.

Zong-Xing, L., Qi, F., Wei, L., Tingting, W., Xiaoyan, G., Zongjie, L., Yan, G., Yanhui, P., Rui, G., Bing, J., Yaoxaun, S., & Chuntan, H. (2015). The stable isotope evolution in Shiyi glacier system during the ablation period in the north of Tibetan Plateau, China. *Quaternary International*, *380–381*, 262–271. https://doi.org/10.1016/j.quaint.2015.02.013

1440   Zou, X., Bromwich, D. H., Montenegro, A., Wang, S. H., & Bai, L. (2021). Major surface melting over the Ross Ice Shelf part II: Surface energy balance. *Quarterly Journal of the Royal Meteorological Society*, *147*(738), 2895–2916. https://doi.org/10.1002/qj.4105

Zuhr, A. M., Münch, T., Steen-Larsen, H. C., Hörhold, M., & Laepple, T. (2021). Local-scale deposition of surface snow on the Greenland ice sheet. *The Cryosphere*, *15*(10), 4873–4900. https://doi.org/10.5194/tc-15-4873-2021